



26 **Abstract**

27 As the level of vehicle automation increases, drivers are more likely to engage in non-driving  
28 related tasks which take their hands, eyes, and/or mind away from the driving task.  
29 Consequently, there has been increased interest in creating Driver Monitoring Systems (DMS)  
30 that are valid and reliable for detecting elements of driver state. Workload is one element of  
31 driver state that has remained elusive within the literature. Whilst there has been promising  
32 work in estimating mental workload using gaze-based metrics, the literature has placed too  
33 much emphasis on point estimate differences. Whilst these are useful for establishing whether  
34 effects exist, they ignore the inherent variability within individuals and between different  
35 drivers. The current work builds on this by using a Bayesian distributional modelling approach  
36 to quantify the within and between participants variability in Information Theoretical gaze  
37 metrics. Drivers (N = 41) undertook two experimental drives in hands-off Level 2 automation  
38 with their hands and feet away from operational controls. During both drives, their priority was  
39 to monitor the road before a critical takeover. During one drive participants had to complete a  
40 secondary cognitive task (2-back) during the hands-off Level 2 automation. Changes in  
41 Stationary Gaze Entropy and Gaze Transition Entropy were assessed for conditions with and  
42 without the 2-back to investigate whether consistent differences between workload conditions  
43 could be found across the sample. Stationary Gaze Entropy proved a reliable indicator of  
44 mental workload; 92% of the population were predicted to show a decrease when completing  
45 2-back during hands-off Level 2 automated driving. Conversely, Gaze Transition Entropy  
46 showed substantial heterogeneity; only 66% of the population were predicted to have similar  
47 decreases. Furthermore, age was a strong predictor of the heterogeneity of the average causal  
48 effect that high mental workload had on eye movements. These results indicate that, whilst  
49 certain elements of Information Theoretic metrics can be used to estimate mental workload by  
50 DMS, future research needs to focus on the heterogeneity of these processes. Understanding

51 this heterogeneity has important implications toward the design of future DMS and thus the  
52 safety of drivers using automated vehicle functions. It must be ensured that metrics used to  
53 detect mental workload are valid (accurately detecting a particular driver state) as well as  
54 reliable (consistently detecting this driver state across a population).

55 Keywords: Distraction, workload, DMS, heterogeneity, automation, entropy

56

57

58

59

60

61

62

63

64

65

66

67

68

## 69 1 Introduction

70 The influx of automated systems in road vehicles has generated increased interest in the  
71 development of Driver Monitoring Systems (DMS). DMS refers to a collection of sensors that  
72 aim to detect whether a driver is attentive, alert, or engaged. Not only are drivers more likely  
73 to engage in non-driving related tasks (NDRTs) as vehicles transform from manual to partial  
74 driving automation (Carsten et al, 2012), but in Level 3 automation drivers are allowed to  
75 actively engage in NDRTs (SAE, 2018). This may take their hands off the wheel and eyes and  
76 mind away from the main driving task. As such, a large body of research has aimed to measure  
77 the internal states of drivers whilst using partial or conditionally automated vehicles, and how  
78 these states might change in response to NDRTs. One elusive, yet extremely relevant, driver  
79 state for informing driver readiness is workload. Workload is a general term that can be defined  
80 as the demand or difficulty that is placed upon a driver (De Waard, 1996; da Silva, 2014; Fuller,  
81 2005; De Winter et al, 2014). *Mental workload* is more specific and has been defined as the  
82 proportion of information processing for a given task relative to an individual's processing  
83 capacity (Brookhuis & De Waard, 1993; 2000; da Silva, 2014). It should also be noted that the  
84 terms *cognitive distraction* and *cognitive load* are often used interchangeably when researchers  
85 manipulate the cognitive demand of drivers. However, there is a distinct conceptual difference;  
86 the former referring to the general removal of attention away from the driving task toward a  
87 secondary task, and the latter referring to the quantity of the cognitive resource demanded by  
88 the secondary task (Engström et al, 2017). A key aspect of mental workload is that drivers have  
89 a limited pool of cognitive resources (Wickens, 2002). Underload from the monotony of  
90 monitoring autonomous systems can result in decreased vigilance (Young & Stanton, 2002)  
91 whereas overload may occur if a driver is engaging in an NDRT and can result in sub-optimal  
92 takeover performance (Gold et al, 2015; Zeeb et al, 2016). To ensure that a driver is ready to  
93 resume control, they should ideally have moderate workload levels to reduce the likelihood of

94 safety-critical situations (Bruggen, 2015). Hence one goal of DMS development has been to  
95 identify valid and reliable indicators of mental workload to monitor the driver during automated  
96 driving. Therefore, a specific aim of this manuscript was to investigate a family of gaze-based  
97 metrics that have shown potential in estimating mental workload in human drivers.

98 The dispersion of gaze has been a useful metric for measuring mental workload during manual  
99 and automated driving. Gaze dispersion is often measured as the standard deviation of raw gaze  
100 coordinates in the horizontal and vertical dimensions (Sodhi et al, 2002). During manual  
101 driving, the standard deviation of horizontal gaze reduces when the workload of the driver is  
102 increased with a secondary cognitively loading task; this phenomenon is known as visual  
103 tunneling (Reimer, 2009; Reimer et al, 2010; Wang et al, 2014). Similar effects have been  
104 observed when performing a cognitive loading secondary task during automated driving  
105 (Radlmayr et al, 2019; Wilkie et al, 2019). The sensitivity of raw gaze dispersion for detecting  
106 mental workload has proven to be a robust measure for driver monitoring systems. However,  
107 one limitation of this approach is that it does not account for the predictive nature of eye  
108 movements. Established accounts of gaze control focus on the where (spatial distribution) and  
109 the when (temporal sequence) of gaze, relative to task demands (Shiferaw et al, 2019). This is  
110 can be interpreted as being driven by bottom-up (stimulus saliency) or top-down (behavioral  
111 requirements) processes (Henderson, 2003; Shiferaw et al, 2019). However, a growing body of  
112 literature has proposed that gaze control is a system of spatial prediction (Henderson, 2017;  
113 Talter et al, 2017). Hence fixation locations are not merely instructed by top-down and bottom-  
114 up influences, but their relative contributions towards prediction and error correction when  
115 constructing an internal representation of a visual scene (Parr & Friston 2017; Spratling et al,  
116 2017; Shiferaw et al, 2019). The brain is a prediction machine and aims to minimize error  
117 between sensory information and the internal state (Clark et al, 2013). Hence via a combination  
118 of bottom-up and top-down processes, gaze control aims to optimize visual sampling in order

119 to make better predictions regarding the location of subsequent fixations (Parr & Friston, 2017;  
120 Spratling et al, 2017). Considering the mechanisms involved in gaze control, it can be argued  
121 that measuring differences in visual scanning behaviour during varying stages of driving may  
122 provide information on changes in the underlying processes that are influenced by increased  
123 workload (Shiferaw et al, 2019). Information Theoretic concepts such as entropy are one such  
124 method, which focus on using gaze transitions to estimate internal states.

125 Gaze entropy is an eye tracking metric that has shown promise for estimating mental workload  
126 and refers to the application of Information Theory to gaze data (Shiferaw et al, 2019). Within  
127 the field of Information Theory, entropy refers to the average amount of information or  
128 uncertainty for a given choice (Shannon, 1948). For a system with discrete processes, the two  
129 primary components are the source and output; the source being the total number of states that  
130 a given output can take. When applied to gaze data, there is an assumption that saccadic  
131 movements that produce fixations are outputs from a gaze control system that predicts the  
132 spatial locations of proceeding fixations (Shiferaw et al, 2019). The visual field represents all  
133 possible state spaces where a fixation could be located. To calculate the entropy of gaze  
134 fixations, fixation coordinates are divided into discrete spatial bins to generate probability  
135 distributions of a given fixation being within a given location (Shiferaw et al, 2019). The  
136 entropy value thus represents the predictability of a fixation location; a higher uncertainty (or  
137 entropy) represents a higher dispersion of gaze for a particular viewing period (Holmqvist et  
138 al, 2011). This is known as *Stationary Gaze Entropy* ( $H_s$ ). Another assumption is that  
139 subsequent fixations are better predicted by current fixations via *conditional* probability rather  
140 than only *total* probability (Weiss et al, 1989; Shiferaw et al, 2019). Therefore, this provides a  
141 measure of predictability of visual scanning patterns by considering the order of fixations; this  
142 is known as *Gaze Transition Entropy* ( $H_t$ ). Higher  $H_t$  is indicative of less structured, more  
143 random scanning patterns (Shiferaw et al, 2019). Because eye movements aim to optimize

144 inference through motor action sequences (Parr & Friston, 2017), it has been proposed that  
145 there is an optimal range of  $H_t$  to efficiently sample information within the visual scene.  
146 Optimal  $H_t$  is an ideal level of complexity that balances modulation from underlying bottom-  
147 up influences with top-down prediction (Shiferaw et al, 2019). If there is an optimal range of  
148  $H_t$  then *increased*  $H_t$  may reflect top-down interference whereby there is modulation of gaze  
149 beyond the requirements of a given task. This can manifest as highly erratic, random visual  
150 scanning. Conversely, lower than optimal  $H_t$  can result in insufficient top-down modulation  
151 thus producing insufficient visual scanning and exploration. Whilst  $H_t$  may change as a  
152 function of more visually demanding tasks or visual scenes, given an environment where these  
153 factors are experimentally controlled,  $H_t$  may change as a function of top-down engagement  
154 (Shiferaw et al, 2019).

155  $H_s$  and  $H_t$  provide a quantitative assessment of visual scanning in naturalistic environments  
156 and thus have been proposed as measures that can estimate mental workload in drivers. Testing  
157 the reliability and validity of gaze entropic metrics has largely been conducted within the  
158 domain of manual driving. Schieber & Gilland (2008) found reductions in  $H_t$  as a function of  
159 secondary task load difficulty; this was further exacerbated for older drivers. The combination  
160 of older drivers having reduced visual-spatial processing resources alongside the increased  
161 demands of the secondary task resulted in this interaction effect. Schieber & Gilland (2008)  
162 proposed that metrics based on Information Theory held significant potential for monitoring  
163 driver behaviour as  $H_t$  systematically changed as a function of increased mental workload.  
164 Pillai et al (2022) implemented a similar design to investigate whether gaze entropy  
165 differentiated varying levels of cognitive load during manual driving. By calculating the signal-  
166 to-noise ratio (SNR), Pillai et al (2022) found that  $H_s$  reliably differentiated between a control  
167 task (normal driving and a detection response task) and 2-back, control and 0-back, and 0-back  
168 and 2-back conditions. Conversely,  $H_t$  could not reliably distinguish between any of these

169 cognitive load comparisons. This suggests that it was the predictability of the dispersion of  
170 gaze, rather than gaze transitions, that was useful for estimating mental workload. One of the  
171 only experiments to study cognitive load estimation using gaze entropy during automated  
172 driving was conducted by Chen et al (2022). They investigated whether  $H_s$  changed as a  
173 function of automation level (SAE L0, L1, and L2). 3-dimensional  $H_s$  (applying the Shannon  
174 (1948) equation to coordinates in a 3-dimensional plane) negatively correlated with subjective  
175 workload during visual, auditory, or multi-modality cognitive tasks. This is indicative of gaze  
176 dispersion decreasing as a function of increased subjective workload, and thus supports similar  
177 findings of visual tunneling when cognitively loaded (Radlmayr et al, 2019; Reimer, 2009;  
178 Reimer et al, 2010; Wang et al, 2014; Wilkie et al, 2019). Chen et al (2022) concluded that  $H_s$   
179 could be a valid indicator for visual and auditory task distractions within driver monitoring  
180 systems during partial automation.

181 Despite evidence that gaze entropy measures can be useful for estimating mental workload,  
182 there are some limitations to this work. Chen et al (2022) utilized a desktop computer simulator  
183 where the keyboard was used for steering and pedal operations. There was also no simulated  
184 traffic or road; just a highly artificial virtual environment. Not only is this a poor replication of  
185 real driving, but the lack of stimuli within the visual scene may have produced insufficient  
186 bottom-up saliency. There was also no control condition without a secondary task, thus not  
187 allowing for any comparison of gaze entropy under normal workload situations. A wider  
188 limitation of the literature is the lack of investigation into the variation both within and between  
189 individuals. A metric that estimates mental workload must be valid (i.e., the metric  
190 systematically varies with mental workload) but it must also be reliable (i.e., the metric  
191 systematically changes in similar ways for a given population) if it is to be used in DMS within  
192 a wider population. Therefore, understanding how  $H_s$  and  $H_t$  vary is vitally important. Whilst  
193 mean differences are theoretically useful for establishing the existence of effects, they only



194 existence in an abstract sense (Mole et al, 2020). To make applied predictions that relate to the  
195 wider population, it is vital to model and understand how a sample varies. Schieber & Gilland  
196 (2008) reported no indices of variance in  $H_t$ , thus providing no indication as to how variable  
197  $H_t$  was when drivers were under high mental workload. Chen et al (2022) reported large  
198 individual differences in the difficulty of the spatial N-back task which may have influenced  
199 subjective ratings of mental workload alongside eye tracking metrics. However, they did not  
200 formally model these differences, or investigate whether specific individual characteristics  
201 predicted this variation. Finally, Pillai et al (2022) investigated the effects of gaze entropy by  
202 calculating SNR; a lower SNR indicates that two means are more similar. Not only is this  
203 metric focused on mean differences but averages of gaze entropy in different conditions are  
204 weighted by variance across several participants. Whilst this accounts for variation in entropy,  
205 it treats all individual differences as noise. Whilst some individual variance is undoubtedly  
206 attributed to noise in eye tracking measurement (Bottos & Balasingam, 2020; Velichkovsky et  
207 al, 1997), it is possible that individual differences could vary as function of theoretically useful  
208 variables (e.g., age, driving experience).

209 The aim of the current study was to investigate the feasibility of using gaze entropic metrics to  
210 estimate mental workload whilst monitoring a Level 2 automated vehicle with their hands and  
211 feet away from operational controls. Previous research has shown that eye movements change  
212 as a function of increased mental workload (Radlmayr et al, 2019; Reimer et al, 2009; Reimer  
213 et al, 2010; Wilkie et al, 2019). However, using Information Theory to study gaze metrics can  
214 go beyond understanding the spatial distribution of gaze and focus on how efficiently drivers  
215 are scanning the visual scene. Thus far, there is evidence that  $H_s$  and  $H_t$  can be used to detect  
216 driver workload (Chen et al, 2022; Pillai et al, 2022; Schieber & Gilland, 2008). However, the  
217 methodology used to make these conclusions has seemingly ignored how these variables vary  
218 within a given population. Such variance is vital, if we are to understand whether these

219 Information Theoretic metrics can be used by DMS to improve the safety outcomes for a wide  
220 range of users.

## 221 **2 Material and methods**

### 222 2.1 Participants

223 41 participants were recruited from a university participant pool and took part in the experiment  
224 however three had to be removed before data analysis as they either did not follow experimental  
225 instructions, or eye tracking data was not correctly captured. The remaining 38 participants (16  
226 females, 22 males, mean age = 38.81, range = 22-65) all had normal or corrected to normal  
227 vision. All participants had a valid UK driving license (mean number of years = 17.8, range =  
228 4-43) and were regular drivers (mean annual miles = 9355.25, range 5000-20000).

### 229 2.2 Apparatus and materials

230 The experiment was conducted at the University of Leeds Driving Simulator (see Figure 1).  
231 This is a motion-based driving simulator consisting of a Jaguar S-type cab encased within a 4  
232 m spherical projection dome. The dome has a 300° field of view projection to render the driving  
233 environment. Driver controls are fully operational; pedals and steering provide haptic feedback  
234 for participants to replicate real-world driving. Longitudinal and lateral movement is also  
235 provided via a hexapod motion base and a 5 m x 5 m X-Y table. Gaze data were collected using  
236 a Seeing Machines Driver Monitoring System eye tracker sampling at 60 Hz. Subjective ratings  
237 of workload were measured via the NASA-Task Load Index (NASA-TLX). The NASA-TLX  
238 consists of 6 subscales that measure subjective ratings of mental, physical, and temporal  
239 demands as well as frustration, effort, and performance of the task (Hart, 2006).

240  
241  
242  
243  
244  
245  
246  
247  
248  
249  
250  
251  
252  
253  
254  
255  
256  
257  
258  
259  
260  
261  
262



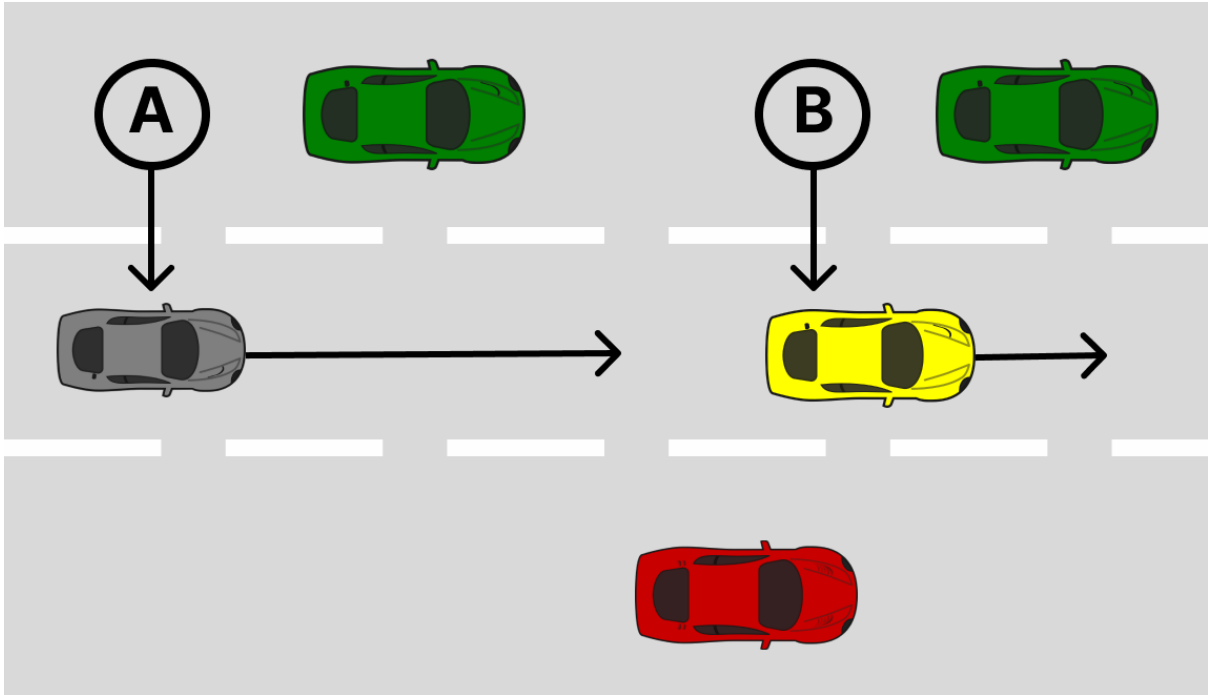
Figure 1: University of Leeds Driving Simulator

### 2.3 Design

A 2 x 2 Repeated Measures design was used in this study. The two within-participant factors were event criticality and mental workload. Event criticality was manipulated by changing the time to collision at the onset of a lead vehicle braking (TTC) after a period of hands-off Level 2 automated driving. The aim of manipulating this variable was to create two levels of criticality: a “less severe” level (TTC = 5 s) that allowed participants to successfully take over without crashing, and a “severe” level that could lead to a crash if the participant was not monitoring the road correctly (TTC = 3 s). These values were chosen based on previous studies that have demonstrated that a 3 s TTC produces highly critical events, whilst a 5 s TTC provides sufficient time for takeovers (Gold et al, 2013; Mok et al, 2015; Louw & Merat, 2017). The second within-participants factor that was manipulated was mental workload. This was manipulated over two levels; a no-load condition and a high mental workload condition where participants had to complete a secondary task during the automated driving sections. To induce cognitive load, participants completed a verbal response delayed digit recall task (N-back) (Mehler et al, 2011) during the automated driving sections. The specific N-back used in the

263 current investigation was a 2-back condition. This task was chosen because it is highly  
264 controlled, non-visual, and has been consistently shown to increase the workload of drivers  
265 during manual (Reimer, 2009; Reimer et al, 2010; Wang et al, 2014) and automated driving  
266 (Radlmayr et al, 2019; Wilkie et al, 2019).

267 The experiment consisted of two drives for each participant. During one drive participants  
268 completed an N-back throughout the automated period; during the other drive there was no  
269 secondary task. The order of N-back was counter-balanced across participants. Each drive  
270 lasted approximately 35 minutes and all participants drove on the same 3-lane UK motorway.  
271 Each drive consisted of 10 discrete events, each consisting of 30 s of manual driving followed  
272 by approximately 2 minutes of automated driving. After 2 minutes of automated driving, a  
273 takeover request (TOR) was delivered. Four of these events were critical: two with a TTC of 3  
274 s, two with a TTC of 5 s. For 3 s TTCs, the lead vehicle braked suddenly and decelerated at a  
275 rate of  $5.55 \text{ m/s}^2$ , whereas for the 5 s event, the lead vehicle decelerated at  $2 \text{ m/s}^2$ . Decelerations  
276 began as soon as the takeover request (TOR) was triggered. The remaining six events were  
277 non-critical; two involved no lead vehicle, and the remaining four involved a lead vehicle that  
278 did not decelerate once the TOR was triggered. Lead vehicles appeared in front of the ego  
279 vehicle shortly before the automation was engaged. They entered the middle lane from the left-  
280 hand lane and participants were instructed to allow the lead vehicle to pull in front. Once in the  
281 middle lane, lead vehicles matched the ego-vehicle's speed at a distance of 25 m during  
282 automation. Participants drove in the middle lane, with ambient traffic flow in the left and right  
283 lanes. Once the lead vehicle was present, the automated system engaged.



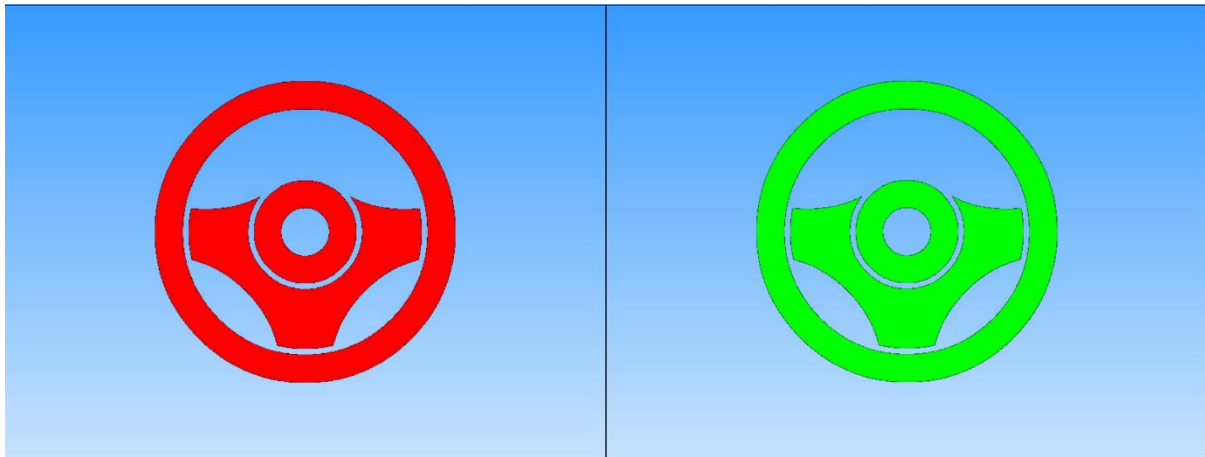
284 *Figure 2: Schematic representation of an event. (A) represents the ego vehicle and (B)*  
 285 *represents the lead vehicle. Lead vehicles entered from the left lane and matched the ego*  
 286 *vehicles speed at a distance of 25 m. Following 2 minutes of automated driving, for critical*  
 287 *trials the lead vehicle decelerated at  $5.55 \text{ m/s}^2$  ( $TTC = 3 \text{ s}$ ) or  $2 \text{ m/s}^2$  ( $TTC = 5 \text{ s}$ ). For non-*  
 288 *critical trials, a TOR was delivered but the lead vehicle did not decelerate.*

#### 289 2.4 Procedure

290 Informed consent was obtained, and standardized procedural instructions were delivered. All  
 291 procedures were approved by the University of Leeds Research Ethics Committee (Reference  
 292 code: 2022-0353-206).

293 Upon arrival participants completed a number of pre-drive questionnaires (data from these  
 294 questionnaires are not analysed or reported in this manuscript). Participants conducted a  
 295 practice session to become familiar with all aspects of the experiment and the driving simulator  
 296 dynamics. Participants were talked through the design of the Human-Machine Interface (HMI)  
 297 (see Figure 3), how to disengage the automation, and completed a static N-back task. During

298 the driving portion of the practice the 3-lane motorway contained ambient traffic. Takeovers  
299 during the practice were non-critical.



300 *Figure 3: Icons used to indicate system status. Green steering wheels indicated the Level 2*  
301 *autonomous system was activated. Red steering wheels indicated that the driver needed to take*  
302 *over. During manual driving, the steering wheel was greyed out. In the experiment, the red*  
303 *steering wheel flashed until the vehicle was back into manual driving mode.*

304 For experimental drives, participants were instructed to enter the motorway and position  
305 themselves in the centre of the middle lane and maintain a speed of 70 MPH. After  
306 approximately 30 s of manual driving the automated system engaged automatically. This was  
307 indicated by a short auditory tone and the shifting of the steering wheel icon from grey (manual  
308 mode) to green (automation engaged) (see Figure 3). Once in automated driving mode,  
309 participants were instructed to take their hands off the wheel and feet away from the pedals and  
310 to monitor the road environment for any potential hazards. After approximately 2 minutes of  
311 automated driving, a TOR was delivered. The TOR was characterised by an auditory tone and  
312 the steering icon flashing red within the instrument cluster. Participants were instructed to take  
313 over once the TOR had been issued; this could be done by any steering input over 2°, pressing  
314 any of the pedals, or pressing a micro-switch button strapped to the steering wheel. If the driver  
315 of the ego-vehicle did not respond within 10 seconds, the automation would disengage by itself.

316 Following the takeover, the participant engaged in 30 s of manual driving before the automated  
317 system engaged once more. If the driver exited the middle lane during takeovers, they were  
318 instructed to return as soon as possible. There were 10 discrete events per drive and each drive  
319 lasted approximately 35 minutes. During one drive participants completed an auditory-verbal  
320 N-back task when automation was engaged, which continued until a TOR was given.  
321 Participants were instructed that a safe drive was their primary goal. After each drive,  
322 participants filled out a NASA-TLX to collect data on subjective ratings of workload. After the  
323 second experimental drive, participants completed post-drive questionnaires (data from these  
324 questionnaires is not analysed or reported in this manuscript).

## 325 2.5 Statistical modelling

326 The main aim of this manuscript was to investigate changes in gaze entropic eye metrics during  
327 the 2-minute automation period with and without N-back, and with and without a lead vehicle.  
328 This includes critical and non-critical trials that included a lead vehicle. Thus, data relating to  
329 the takeover and manual driving portions are not analysed within this manuscript. Data and  
330 analysis code can be found in the following link  
331 ([https://github.com/courtneygoodridge/gaze\\_entropy\\_heterogenous](https://github.com/courtneygoodridge/gaze_entropy_heterogenous)).

### 332 2.5.1 Gaze entropy

333 To calculate stationary gaze entropy ( $H_s$ ), the Shannon (1948) entropy equation was applied to  
334 the fixation data:

$$H_s(x) = - \sum_{i=1}^N p(i) \log_2 p(i) \quad (1)$$

335 Where  $H_s$  is entropy for a given set  $x$  (time period during automation for a given condition),  $i$   
336 is the number of state spaces or locations (in a 2-dimensional coordinate plane) of each fixation  
337 in  $x$ ,  $N$  is the total number of fixations in  $x$ , and  $p(i)$  is the proportion of fixations landing in a

338 given state space. Gaze transition entropy ( $H_t$ ) was calculated by applying the conditional  
339 entropy equation to 1<sup>st</sup> order Markov fixations transitions:

340

$$H_t(x) = - \sum_{i=1}^N p(i) \left[ \sum_{j=1}^N p(i | j) \log_2 p(i | j) \right], i \neq j \quad (2)$$

341

342 When  $p(i)$  is the stationary distribution of fixations,  $p(i | j)$  is the probability of transitioning  
343 to state  $j$  given being currently in state  $i$ , and  $i \neq j$  excludes transitions that occur within the  
344 same state space (Ellis & Stark, 1986). Fixations were split into spatial bins to apply the  
345 equations. This is the primary method of discretisation in the literature (Di Stasi et al, 2017;  
346 Krejtz et al, 2014; 2015, Raptis et al, 2017) and has been proposed as the superior method for  
347 dynamic stimuli (Shiferaw et al, 2019). For interpretability, both  $H_s$  and  $H_t$  were normalized  
348 by dividing by the maximum entropy,  $H_{max}$ . Maximum entropy is the logarithm (base 2) of all  
349 state spaces and thus represents when distributional information is at a maximum. For example,  
350 each fixation is equally spaced out within the visual scene, and each transition is completely  
351 random (Shiferaw et al, 2019). As such,  $H_s$  and  $H_t$  range from 0-1 and represent the percentage  
352 of maximum possible entropy.

### 353 2.5.2 Analytic approach

354 To develop human-centred driver monitoring systems that can reliably detect the mental  
355 workload of drivers, it is important to consider the distribution of driver responses rather than  
356 focusing merely on the mean. Whilst mean differences are useful for establishing the presence  
357 of effects across conditions, using mean values is limited, since it only exists in an abstract  
358 sense - no single driver can be considered “the average” (Mole et al, 2020). Furthermore, means  
359 do not contain *within* or *between individual* variability which are vital components for making



360 real world predictions about human behaviour. Standard regression-based analyses aim to  
361 model the population mean ( $\mu$ ) whilst assuming that the within-participants variance ( $\sigma$ ) is  
362 consistent. Not only is the assumption of homogeneity of variance often violated (Schielzeth  
363 et al, 2020) but there is also theoretical justification that  $\sigma$  might vary as a function of the  
364 manipulated variables in the experiment.

365 As highlighted in the Introduction, the motor coordination of eye movements aims to optimise  
366 inference (Parr & Friston, et al 2017). This implies that there is an optimal level of  $H_t$  for  
367 effective sampling of the visual scene whereby top-down processes modulate default bottom-  
368 up activation (Shiferaw et al, 2019). Whilst increases or decreases in the  $\mu$  of  $H_t$  can be  
369 indicative of top-down interference or top-down modulation respectively (Shiferaw et al,  
370 2019), the trial-by-trial variance within individuals can also be a crucial index for measuring  
371 the efficiency of visual scanning. Under the assumption that the visual scene maintains an  
372 ambient level of complexity, optimal  $H_t$  should be consistent within an individual. However,  
373 if increased mental workload results in decreases in  $H_t$  via top-down modulation, it may also  
374 affect how efficiently individuals are able to maintain optimal  $H_t$  from one trial to the next.  
375 The idea that a change in *variance* can indicate a change in a driver's internal state is not new  
376 within the driver monitoring and distraction literature. Horrey & Wickens (2007) proposed that  
377 standard statistical methods that focus on mean differences (or other measures of central  
378 tendency) are insufficient for measuring driver distraction, and that modelling large deviations  
379 in attention can reveal infrequent lapses in visual sampling control; something that can be  
380 missed when only focusing on averages. Kujala & Saarilouma (2011) found reductions in the  
381 standard deviation of fixation durations for simpler in-vehicle information systems menu  
382 designs, thus suggesting that the variance in fixations durations could be used to assess the  
383 efficiency of visual search performance. It is thus proposed in this manuscript that a similar  
384 effect might be present for  $H_t$  , when increasing mental workload. To assess whether there are

385 systematic changes in  $\sigma$  as a function of the predictor variables, the current analysis will apply  
386 distributional models. Distributional models relax the assumption of consistent  $\sigma$ , and allow it  
387 to be predicted by parameters as can be done when predicting  $\mu$  (Bürkner, 2017).

388 It is also vital to quantify *between-participants variance*, as the overall aim of any analysis is  
389 to make predictions towards the population. This is particularly true for DMS, if these systems  
390 are to be reliable for establishing the state of a large and varying driver population. To model  
391 the between-participants variance, we used a multilevel modelling approach. The multilevel  
392 aspect of the model refers to the inclusion of fixed and random effects. Whilst fixed effects  
393 refer to the contribution of a predictor variable towards the average change, random effects  
394 model the variation between different participants on average, alongside how they vary in  
395 response to predictor variables (Lo & Andrews, 2015).

#### 396 2.5.2.1 Model development

397 The population mean,  $\mu$ , of all the gaze-based metrics were modelled as the linear combination  
398 of an intercept ( $\beta_0$ ), N-back ( $N, \beta_N$ ), presence of a lead vehicle ( $L, \beta_L$ ), and an interaction term  
399 between these variables ( $NL, \beta_{NL}$ ). The N-back task was parameterised as  $N \in \{0, 1\}$  where  
400  $N = 1$  corresponds to the presence of the N-back during hands-off Level 2 automation.  
401 Similarly, lead vehicle was parameterised as  $L \in \{0, 1\}$  where  $L = 1$  corresponds to the  
402 presence of a lead vehicle during automation. The standard deviation,  $\sigma$ , was independently  
403 modelled as a linear combination of an intercept ( $\alpha_0$ ), N-back ( $\alpha_N$ ), presence of a lead vehicle  
404 ( $\alpha_L$ ), and an interaction ( $\alpha_{NL}$ ). Because  $\sigma$  cannot be negative, the  $\log(\sigma)$  was modelled. The  
405 distributional model structure was specified as follows:

406

407

$$Y_{ij} \sim N(\mu_{ij}, \sigma_{ij}) \quad (3)$$

$$\mu_{ij} = (\beta_0 + \beta_{0j}) + (\beta_N N_i + \beta_{Nj} N_i) + (\beta_L L_i) + (\beta_{NL} N L_i)$$

$$\log(\sigma_{ij}) = (\alpha_0 + \alpha_{0j}) + (\alpha_N N_i + \alpha_{Nj} N_i) + (\alpha_L L_i)$$

$$\begin{bmatrix} \beta_{0j} \\ \beta_{Nj} \end{bmatrix} \sim MVN \left( \begin{bmatrix} \beta_0 \\ \beta_N \end{bmatrix}, S_\beta \right)$$

$$\begin{bmatrix} \alpha_{0j} \\ \alpha_{Nj} \end{bmatrix} \sim MVN \left( \begin{bmatrix} \alpha_0 \\ \alpha_N \end{bmatrix}, S_\alpha \right)$$

$$S_\beta = \begin{pmatrix} \sigma_{\beta_{0j}}^2 & \rho \sigma_{\beta_{Nj}} \sigma_{\beta_{0j}} \\ \rho \sigma_{\beta_{0j}} \sigma_{\beta_{Nj}} & \sigma_{\beta_{Nj}}^2 \end{pmatrix}$$

$$S_\alpha = \begin{pmatrix} \sigma_{\alpha_{0j}}^2 & \rho \sigma_{\alpha_{Nj}} \sigma_{\alpha_{0j}} \\ \rho \sigma_{\alpha_{0j}} \sigma_{\alpha_{Nj}} & \sigma_{\alpha_{Nj}}^2 \end{pmatrix}$$

408 Where  $Y$  denotes the response variable,  $i$  specifies the condition of each variable,  $j$  specifies  
 409 the participant, and  $S_\beta$  and  $S_\alpha$  are matrices corresponding to the variance or covariance  
 410 parameters.

411 A model was also built to investigate how N-back influenced subjective mental workload. The  
 412 population mean,  $\mu$ , was modelled as linear combination of an intercept ( $\beta_0$ ) and N-back  
 413 (denoted  $N$ ,  $\beta_N$ ):

$$Y_{ij} \sim N(\mu_{ij}, \sigma_{ij}) \quad (4)$$

$$\mu_{ij} = (\beta_0 + \beta_{0j}) + (\beta_N N_i + \beta_{Nj} N_i)$$

$$\begin{bmatrix} \beta_{0j} \\ \beta_{Nj} \end{bmatrix} \sim MVN \left( \begin{bmatrix} \beta_0 \\ \beta_N \end{bmatrix}, S_\beta \right)$$

$$S_\beta = \begin{pmatrix} \sigma_{\beta_{0j}}^2 & \rho \sigma_{\beta_{Nj}} \sigma_{\beta_{0j}} \\ \rho \sigma_{\beta_{0j}} \sigma_{\beta_{Nj}} & \sigma_{\beta_{Nj}}^2 \end{pmatrix}$$

414 Where  $Y$  denotes the response variable,  $i$  specifies the condition of each variable,  $j$  specifies  
415 the participant, and  $S_{\beta}$  is a matrix corresponding to the variance or covariance parameters.

#### 416 2.5.2.2 *Model fitting*

417 A Bayesian approach was used in this manuscript to analyse the data. Posterior distributions  
418 were estimated using the No-U-Turn Sampler (NUTS) in the brms package in the R  
419 programming language (Bürkner, 2017). For parameters estimating mean ( $\mu$ ) differences  
420 between the predictor variables, informative priors were used. For distributional parameters,  
421 brms defaults were used to reflect that  $\sigma$  is a standard deviation and thus can only take positive  
422 values. The final models were reached by incrementally increasing model complexity. Model  
423 comparisons were made using leave-one-out cross validation and additional terms were only  
424 kept if they decreased prediction errors (Vehtari et al, 2017).

425 Using a Bayesian approach, each parameter has an associated probability distribution which  
426 quantifies the level of uncertainty, conditioned on the data. In this manuscript, posterior  
427 distributions of parameters are described by their mean and a 95% Credible Interval (CI)  
428 whereby there is a 95% probability that the true parameter value will fall; values inside this  
429 density have higher credibility than those outside it (Kruschke, 2014). The reader is  
430 discouraged in making dichotomous decisions when understanding whether there is an effect.  
431 Rather, they should use the mean and 95% CIs to assess size, direction, and uncertainty of an  
432 effect. Where appropriate, the *probability of direction* ( $pd$ ) is also reported to illustrate what  
433 percentage of the posterior distribution is above or below 0 (Makowski et al, 2019).

### 434 **3 Results**

#### 435 3.1 Subjective measures

436 To develop a ground truth regarding the cognitive loading effects of the N-back task, the mental  
437 demand facet of the NASA-TLX was compared between N-back conditions. The  $\beta_N$  parameter

438 predicts that the presence of N-back during hands-off Level 2 automated driving doubled  
 439 subjective scores of mental demand on average from 38.994 to 78.705. The model predicts  
 440 with high certainty that N-back produced large increases in subjective mental workload.

441 *Table 1: Posterior means and 95% CIs for fixed effect parameters predicting  $\mu_{ij}$  of NASA TLX*  
 442 *mental demand*

Fixed effects	
Dependent variable:	
<i>Mental demand</i>	
$\beta_0$	38.994 (32.656, 45.257)
$\beta_N$	39.711 (32.057, 47.369)
Participants	38
Observations	76

443

### 444 3.2 N-back performance

445 Performance data for the N-back task was only available for 37 out of 38 participants due to  
 446 data loss. The average performance was reasonably high and homogenous across the sample  
 447 ( $M = 70.77$ ,  $SD = 15.13$ ) however the high and low scores were quite different (range = 37.38  
 448 – 90.97). Previous research in manual driving had found that younger drivers had significantly  
 449 better 2-back performance in comparison to older drivers (Öztürk et al, 2023). To investigate  
 450 this, a univariate Bayesian correlation model was fitted on the standardised values of age and  
 451 performance. The results indicate a negative correlation of  $-.349$  (95% CI:  $-.666$ ,  $-.037$ )  
 452 suggesting that older drivers tended to have worse N-back performance. This medium effect  
 453 size is slightly lower than what was been found in manual driving (Öztürk et al, 2023) although  
 454 the average correlation did highlight a lot of variability; the correlation could be up to  $-.666$ , or  
 455 as low as  $-.03$  (effectively zero).

456

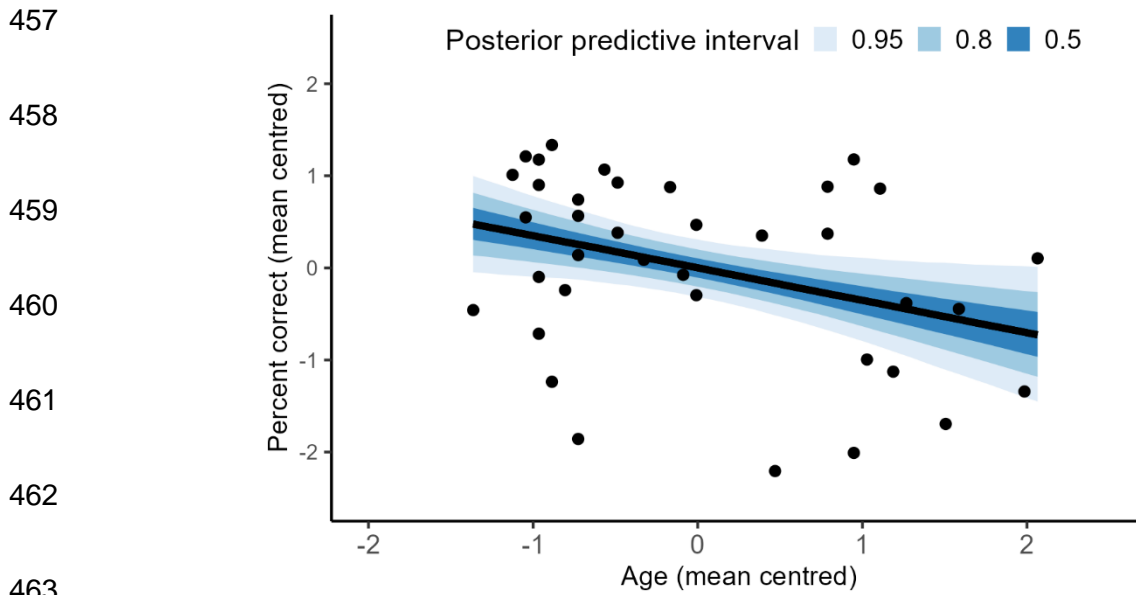


Figure 4: Correlation between age and percentage of correct 2-back responses. Values are standardized to maintain model stability. Black line represents the posterior mean surrounded by bands representing predictive intervals.

### 3.3 Gaze behaviours

Now that it has been established that N-back increased subjective mental workload between the different driving conditions, an investigation into differences in eye movements can be conducted to see if there were reliable differences in gaze entropic metrics as a function of N-back.

#### 3.3.1 Stationary Gaze Entropy ( $H_S$ )

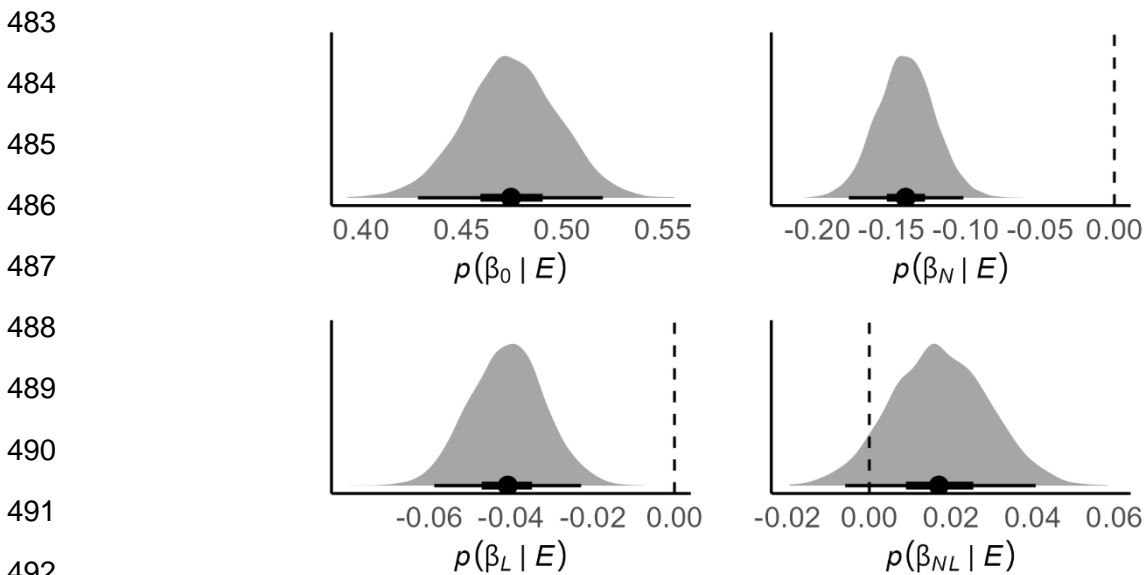
##### 3.3.1.1 Distributional parameters for $H_S$

The  $\beta_N$  parameter predicted an average decrease in  $H_S$  of  $-0.141$  (95% CI:  $-0.178, -0.101$ ) when drivers completed the N-back task; equivalent to a 14 percentage point reduction in normalized  $H_S$ . The  $\beta_L$  parameter predicted an average decrease in  $H_S$  of  $-0.041$  (95% CI:  $-0.058, -0.022$ ) when a lead vehicle was present during automation; equivalent to a 4 percentage point reduction. The  $\beta_{NL}$  parameter was estimated to be  $0.017$  suggesting that N-back reduced the difference in  $H_S$  between lead and no lead conditions by around 1.7 percentage points. However, as highlighted

480 in Figure 5 there is some uncertainty for this effect; only 92% of the most probable parameters  
 481 values are above 0.

482 *Table 2: Posterior means and 95% CIs for fixed effect parameters predicting  $\mu_{ij}$  of  $H_s$*

Fixed effects	
Dependent variable:	
$H_s$	
$\beta_0$	.474 (.428, .520)
$\beta_N$	-.141 (-.178, -.101)
$\beta_L$	-.041 (-.058, -.022)
$\beta_{NL}$	.017 (-.006, .040)
Participants	38
Observations	744



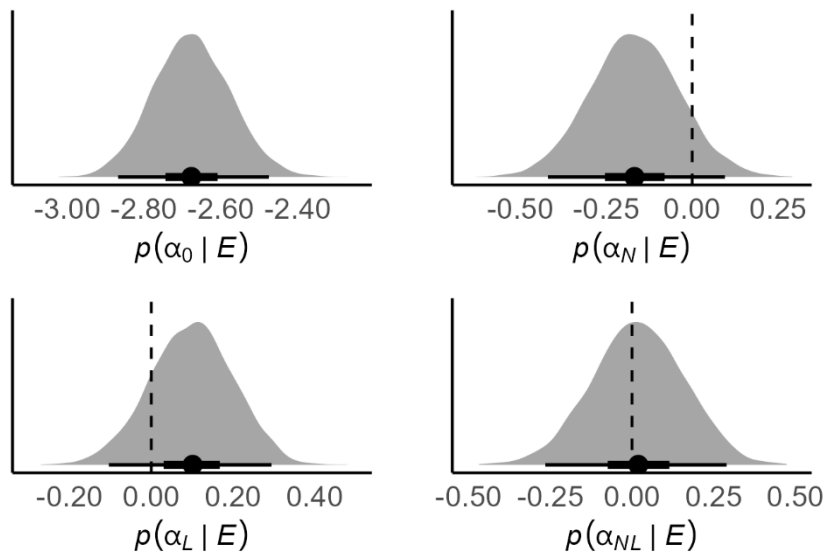
493 *Figure 5: Posterior distributions for model parameters predicting the effect of N-back, lead*  
 494 *vehicle, and their interaction on the  $\mu_{ij}$  of  $H_s$ . N-back and lead vehicle have strong negative*  
 495 *effects on  $H_t$ . The interaction effect is positive, but uncertain with regard to its direction.*  
 496 *Dashed lines are presented to illustrate a null effect.*

497 The direction of the effects for  $\sigma_{ij}$  of  $H_s$  are uncertain. N-back is predicted to decrease  $\sigma_{ij}$  by  
 498 15%, however the probability that the effect is negative is only 90%. As shown in Figure 6, a  
 499 similar pattern of results is found for the presence of the lead vehicle and the interaction effect.

500 Table 3: Posterior means and 95% CIs for fixed effect parameters predicting  $\sigma_{ij}$  of  $H_s$

Fixed effects	
Dependent variable:	
$H_s$	
$\alpha_0$	-2.676 (-2.867, -2.475)
$\alpha_N$	-.167 (-.420, .095)
$\alpha_L$	.098 (-.103, .294)
$\alpha_{NL}$	.019 (-.265, .290)
Participants	38
Observations	744

501



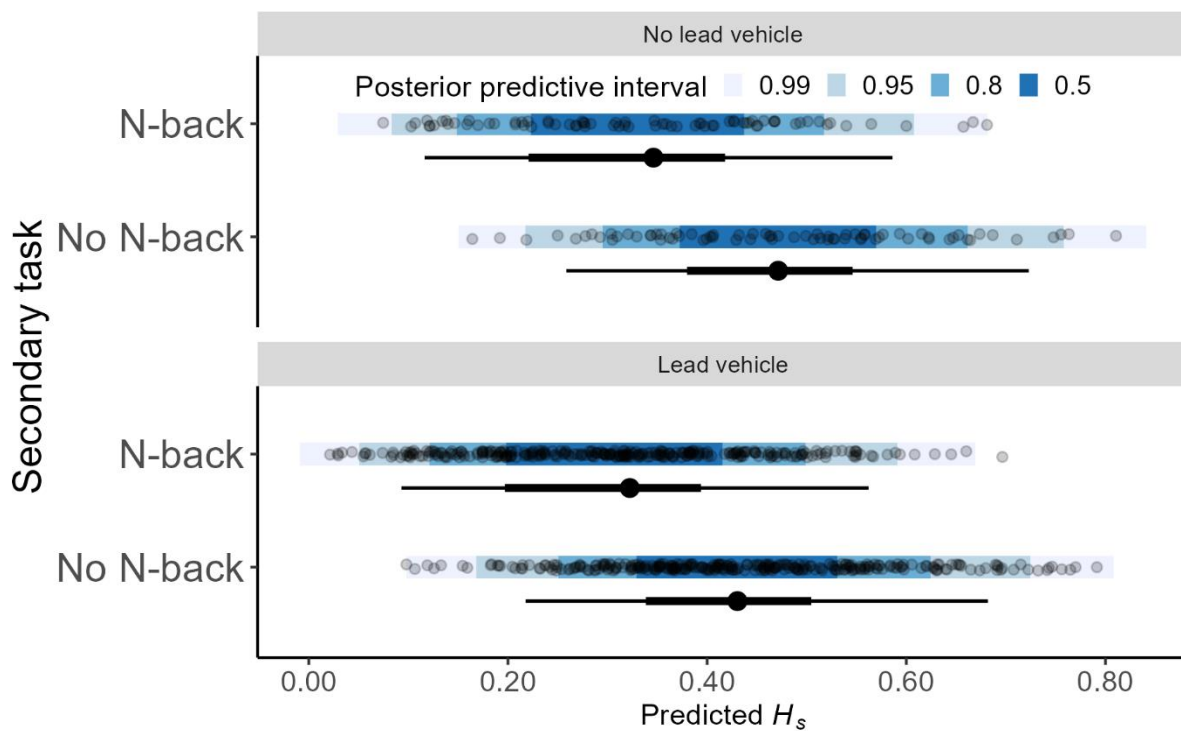
510

511 Figure 6: Posterior distribution for model parameters predicting the effect of N-back, lead  
 512 vehicle, and their interaction, on  $\sigma_{ij}$  of  $H_s$ . The effect of N-back  $\sigma_{ij}$  is estimated to be negative,  
 513 however there is only a 90% probability of this. The effects of lead vehicle and the interaction  
 514 are estimated to be close to 0, thus highlighting high uncertainty with regard to the size and  
 515 direction of their effect on the within-participants variance of  $H_t$ . Dashed lines are presented  
 516 to illustrate a null effect.

517 Overall, the model predicts that N-back reduces the spatial distribution of gaze. This is  
 518 evidence of reduced top-down engagement when monitoring the road environment during  
 519 hands-off Level 2 automated driving. This supports previous research which has shown that



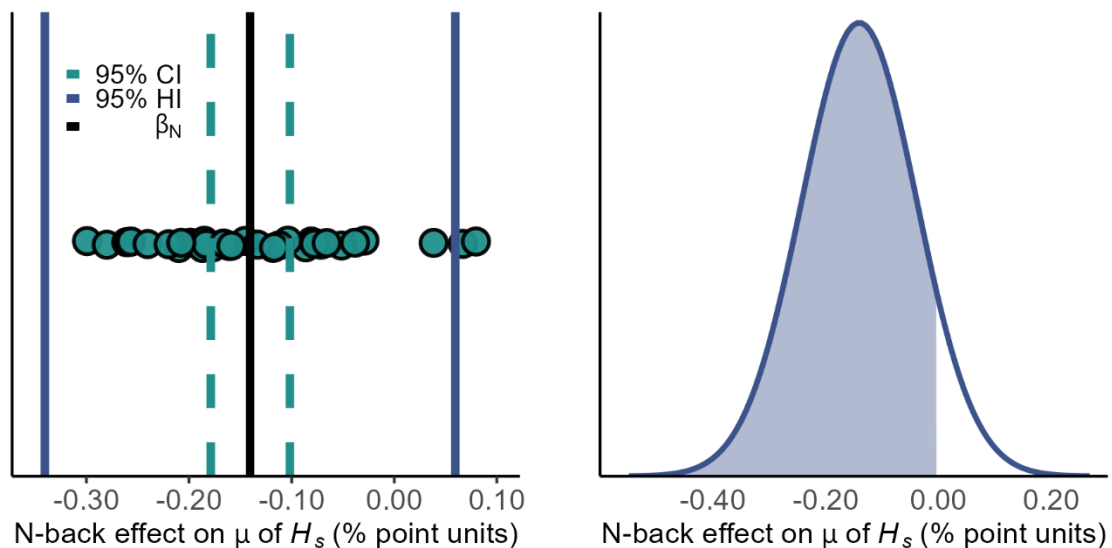
520 increased mental workload during automated driving reduces gaze dispersion (Wilkie et al,  
 521 2019) and suggests that  $H_s$  could be a good metric for estimating mental workload in drivers.  
 522 Modelling the trial-by trial variance in  $H_s$  did not show strong effects of N-back or lead vehicle.  
 523 This is highlighted in Figure 7, whereby the predictive intervals overlayed on raw data have  
 524 similar ranges around their predicted means for all conditions. This suggests that *variance* in  
 525 gaze dispersion from trial to trial was consistent across trials and thus changes in  $\sigma_{ij}$  of  $H_s$  may  
 526 not be useful for detecting increased driver workload.



527 *Figure 7: Posterior predictive bands and posterior distribution of means plotted against raw*  
 528 *data for conditions with and without a lead vehicle. The point-interval plot highlights the*  
 529 *predicted mean differences between N-back/no N-back and lead/no lead vehicle alongside 50%*  
 530 *and 95% credible interval bars. For both lead vehicle and N-back comparisons, the posterior*  
 531 *predictive intervals are roughly of similar size highlighting the lack of evidence for N-back and*  
 532 *lead vehicle affecting  $\sigma_{ij}$  of  $H_s$ .*

533 3.3.1.2 Heterogeneity parameters for  $H_s$

534 Although the typical driver had reduced  $H_s$  by 14 percentage points during the N-back  
535 condition, people differed in the size of this effect. Some participants had reductions as large  
536 as 29 percentage points, some as a low as 3 percentage points, whereas some demonstrated  
537 increases in  $H_s$  by up to 8 percentage points (see Figure 8, left panel). Despite these outlying  
538 participants, the model estimates that 92% of the population are expected to have reductions in  
539  $H_s$  as a result of completing N-back during automation; the remaining 8% of the population  
540 are expected to see moderate increases in  $H_s$  whilst cognitively loaded (see Figure 9, right  
541 panel).



542 *Figure 8: Left panel: strip plot displaying the range of causal effect of N-back on  $H_s$ . The black*  
543 *lines denote the average decrease in  $H_s$  (fixed effect), the blue dashed lines denote the*  
544 *heterogeneity of the average casual effect of N-back (95% Credible Intervals) and the red solid*  
545 *lines denote the population heterogeneity of the effect of N-back. Right panel: population*  
546 *heterogeneity distribution implied by the model estimates of the mean and standard deviation.*  
547 *92% of the population are predicted to demonstrate decreases in  $H_s$  when completing N-back*  
548 *tasks.*

549 These results suggest that  $H_s$  is a strong contender for estimating mental workload during  
 550 hands-off Level 2 automated driving. Reductions in  $H_s$  during N-back are consistent across a  
 551 population, with the model predicting that 92% of the population would have similar decreases  
 552 under similar situations. Although the direction of this effect is consistent, the magnitude can  
 553 vary drastically; up to 2.5 times larger than the average predicted from this sample.

### 554 3.3.2 Gaze Transition Entropy ( $H_t$ )

#### 555 3.3.2.1 Distributional parameters for $H_t$

556 The  $\beta_N$  parameter predicted that the average decrease in  $H_t$  was -.021 (95% CI: -.037, -.004)  
 557 when drivers were completing the N-back task during automated driving. This is equivalent to  
 558 a reduction of 2 percentage points in  $H_t$ . It should be noted that the average effect could be as  
 559 low as a reduction of .004 percentage points which would be effectively 0, or as high as a 3.7  
 560 percentage point reduction. The model parameters for the effect of lead vehicle and the  
 561 interaction between N-back and lead vehicle were estimated as close to 0 with high certainty,  
 562 thus suggesting no meaningful effect on average  $H_t$  (see Table 4).

563 *Table 4: Posterior means and 95% CIs for parameters predicting the  $\mu_{ij}$  of  $H_t$*

Fixed effects	
	Dependent variable:
	$H_t$
$\beta_0$	.215 (.208, .222)
$\beta_N$	-.021 (-.037, -.004)
$\beta_L$	.001 (-.003, .006)
$\beta_{NL}$	-.005 (-.012, .001)
Participants	38
Observations	744

564  
 565  
 566  
 567

568  
569  
570  
571  
572  
573  
574  
575  
576  
577  
578  
579  
580  
581  
582  
583  
584  
585  
586  
587  
588  
589  
590  
591  
592

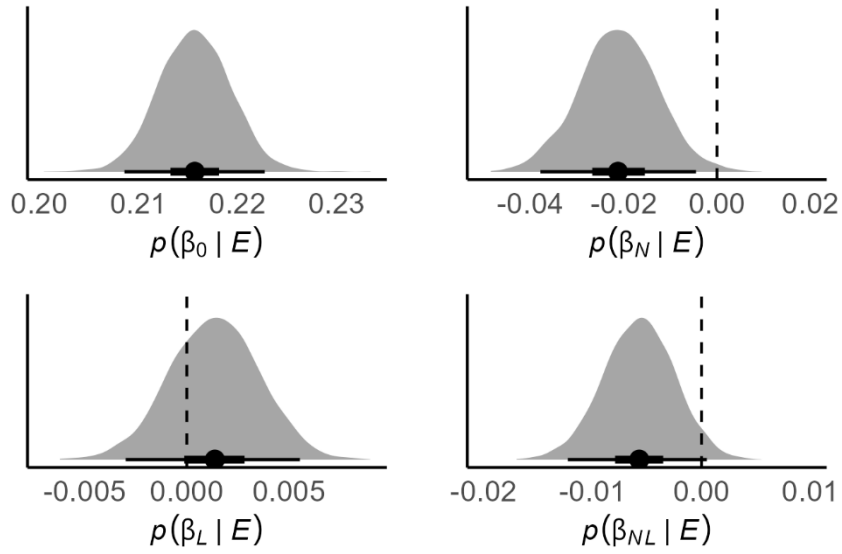


*Figure 9: Posterior distribution for model parameters predicting the effect of N-back, lead vehicle, and their interaction on  $\mu_{ij}$  of  $H_t$ . N-back has a small negative effect on  $H_t$ . The effects of lead vehicle and the interaction are estimated to be close to 0 with reasonably high certainty. Dashed lines are presented to illustrate a null effect.*

The model also predicted differences in the  $\sigma_{ij}$  of  $H_t$  as a function of N-back and lead vehicle (see Table 5). The  $e^{\alpha_N}$  parameter highlights an increase of 44% in within-participants variance in  $H_t$  when completing the N-back during automation. The  $e^{\alpha_L}$  parameter indicates that  $H_t$  increased by 35% when a lead vehicle was present. The  $e^{\alpha_{NL}}$  parameter suggests that the difference in within-participants variance between conditions with and without a lead vehicle were 23% smaller when drivers were not completing the N-back. However, there is some uncertainty with this effect; the probability of the effect being above 0 is 95% (see Figure 10).

593 *Table 5: Posterior means and 95% CIs for parameters predicting the  $\sigma_{ij}$  of  $H_t$*

Fixed effects	
Dependent variable:	
$H_t$	
$\alpha_0$	-4.145 (-4.369, -3.920)
$\alpha_N$	.369 (.042, .696)
$\alpha_L$	.304 (.089, .524)
$\alpha_{NL}$	-.262 (-.568, .040)
Participants	38
Observations	744

594

595

596

597

598

599

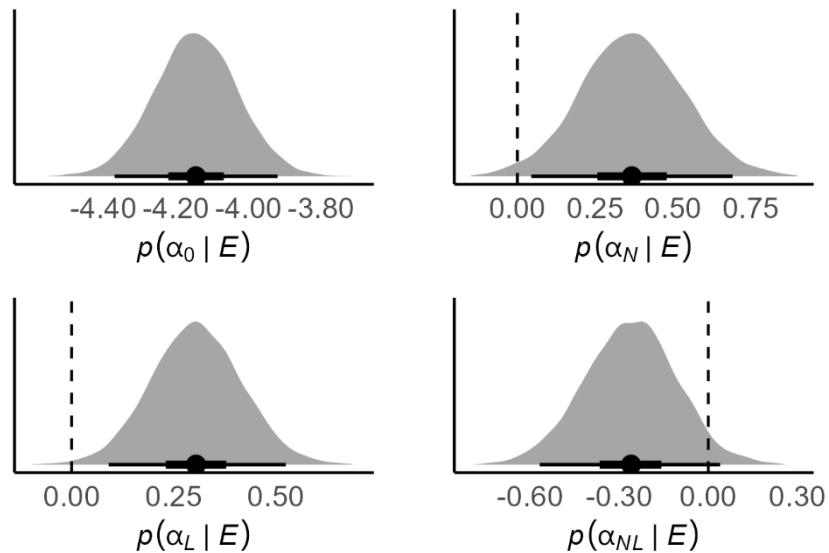
600

601

602

603

604



605

606

607

608

609

610

611

612

*Figure 10: Posterior distribution for model parameters predicting the effect of N-back, lead vehicle, and their interaction, on  $\sigma_{ij}$  of  $H_t$ . N-back and lead vehicle have strong negative effects on  $H_t$ . The interaction effect is negative but slightly uncertain with regard to its direction; only 95% of the posterior distribution is above 0. Dashed lines are presented to illustrate a null effect.*

Model parameters highlight that completing N-back during automated driving produces fixation transitions that are less erratic and more constrained within the visual scene. This average decrease suggests that N-back produced top-down modulation of visual scanning

613 resulting in less complex, more constrained scanning behaviours. The concurrent reduction in  
614 mean  $H_s$  and  $H_t$  as a function of N-back suggests that drivers did not perform sufficient  
615 exploration of the visual scene while under high workload, and thus had reduced top-down  
616 engagement whilst monitoring the automated system. This can be taken as evidence that, on  
617 average, drivers during Level 2 automation who were under high workload had reduced  
618 complexity of eye movements. The model also predicted *increases* in the  $\sigma_{ij}$  of  $H_t$  as a function  
619 of N-back. The increase in  $\sigma_{ij}$  of  $H_t$  is highlighted in Figure 11; raw data are dispersed across  
620 a broader range during N-back conditions. The systematic change in  $\sigma_{ij}$  as a function of N-  
621 back tells us something about the relationship between visual scanning complexity and mental  
622 workload. Not only did drivers have reductions in scanning complexity, but they also failed to  
623 maintain a consistent complexity on a trial-by-trial basis. Instead, drivers demonstrated  
624 frequent fluctuations.

625 The presence of a lead vehicle had no meaningful effect on mean  $H_t$ . However,  $\sigma_{ij}$  did  
626 increased by 35% in the presence of a lead vehicle. This suggests that when following a lead  
627 vehicle, drivers struggled to maintain their scanning complexity within an optimal range;  
628 instead, their trial-by-trial variance in  $H_t$  was high.

629

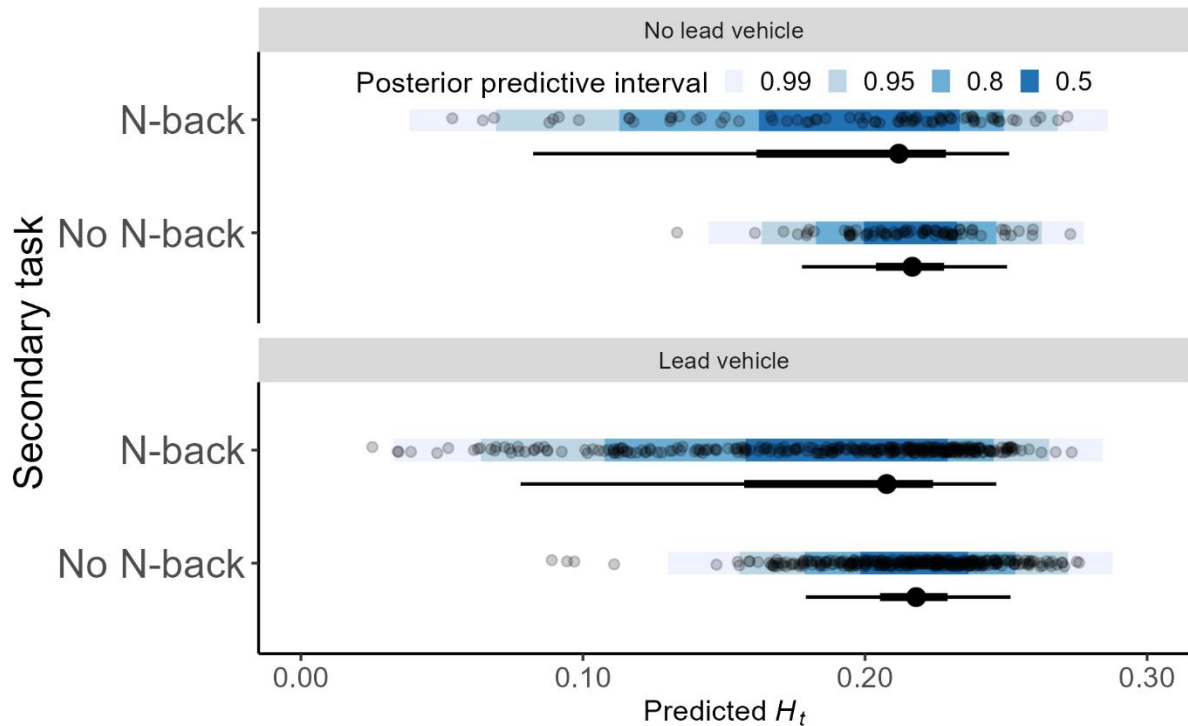
630

631

632

633

634

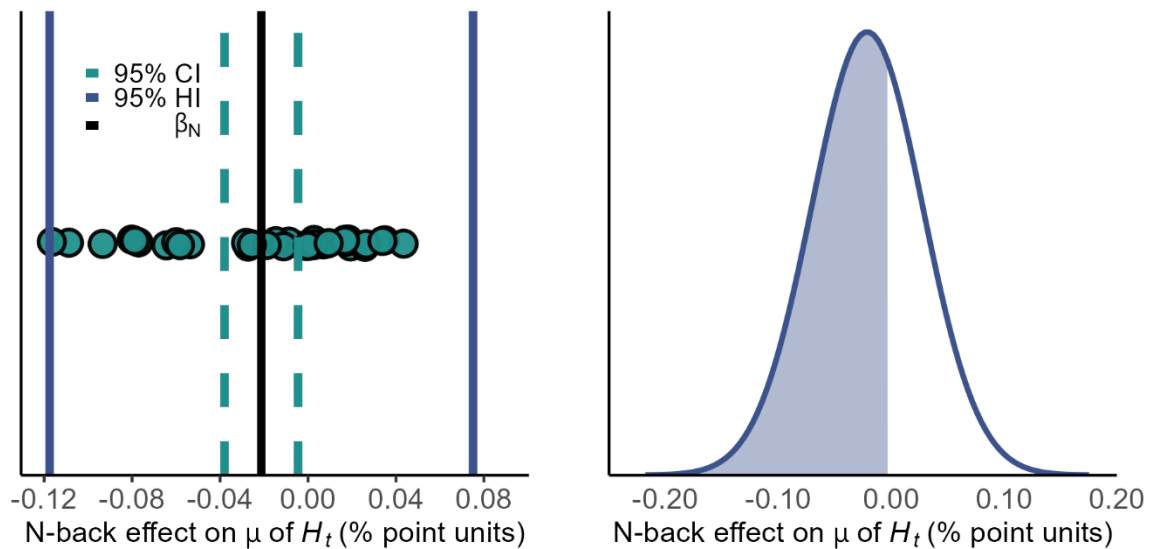


635 *Figure 11: Posterior predictive bands and posterior distribution of means plotted against raw*  
 636 *data for  $H_t$ . The point-interval plot highlights the predicted mean differences between N-*  
 637 *back/no N-back and lead/no lead vehicle alongside 50% and 95% credible interval bars. It is*  
 638 *evident that there are small differences in predicted means between N-back and no N-back,*  
 639 *however lead vehicle seems to have no effect on mean  $H_t$ . It is also evident that  $\sigma_{ij}$  increases*  
 640 *as a function of N-back and lead vehicle, which is highlighted by the wider predictive intervals*  
 641 *and larger spread of the data.*

#### 642 3.3.2.2 Heterogeneity parameters for $H_t$

643 The heterogeneity parameters of the model highlight considerable variance; the random slope  
 644 parameter ( $\beta_{N_j}$ ) is almost two and a half times bigger than the average causal effect ( $\beta_N$ ).  
 645 Whilst the average reduction in  $H_t$  during N-back was 2 percentage points, some people have  
 646 decreases in  $H_t$  of -.125 during N-back (12.5 percentage points) whereas some have *increases*  
 647 of up to .043 (4 percentage points) (see Figure 12, left panel). Furthermore, over 40% of the  
 648 sample show small-to-moderate *increases* in  $H_t$  during the N-back; a reversal of the average

649 trend. This suggests that a considerable proportion of the sample demonstrate more erratic and  
 650 random sampling patterns when cognitively distracted. The model predicts that only 66% of  
 651 the population will show an average decrease in  $H_t$  when completing the N-back during Level  
 652 2 automated driving (see Figure 12, right panel). The remaining 34% of the population are  
 653 expected to show increases in  $H_t$ , resulting in more erratic fixations transitions when  
 654 cognitively loaded.

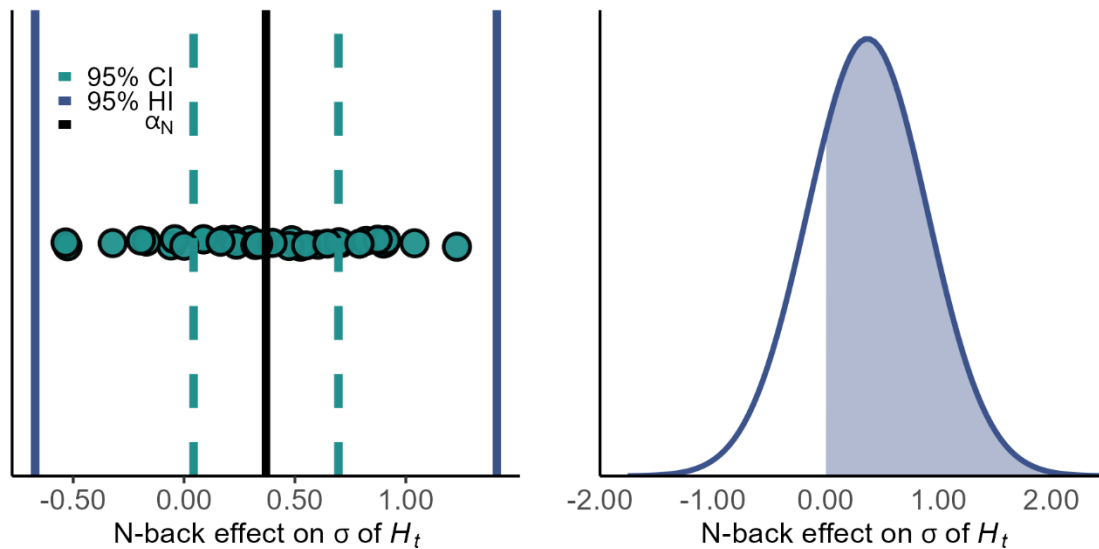


655 *Figure 12 The left panel shows a strip plot of the model predictions of the causal effect of 2-*  
 656 *back on  $H_t$ . The black lines denote the average mean decrease in  $H_t$  (fixed effect), the blue*  
 657 *dashed lines denote the heterogeneity of the average casual effect of N-back (95% Credible*  
 658 *Intervals) and the red solid lines denote the population heterogeneity of the effect of N-back.*  
 659 *The right panel shows the population heterogeneity distribution implied by the model's*  
 660 *estimates of the mean and standard deviation for effect of N-back on  $H_t$ . Only 66% of the*  
 661 *population are predicted to demonstrate mean decreases in  $H_t$  when completing the N-back*  
 662 *task.*

663 Compare this to changes in  $\sigma_{ij}$  of  $H_t$  as a function of N-back. The random slope parameter  
 664 predicting  $\sigma_{ij}$  ( $\alpha_{N_j}$ ) is only 1.5 times bigger than the average causal effect of N-back on  $\sigma_{ij}$



665 ( $\alpha_N$ ). This is further supported by looking at individual changes in  $\sigma_{ij}$  of  $H_t$  as a function of  
 666 the N-back (see Figure 13, left panel). Whilst there is variation in the size of the effect, the  
 667 direction of the effect is more consistent across the sample. This is reflected in the model  
 668 predictions for the population; it predicts that 76% of the population show average increases in  
 669 trial-by-trial variance when completing the N-back task during Level 2 automated driving.



670 *Figure 13: The left panel shows a strip plot of the model predictions of the causal effect of N-*  
 671 *back on  $\sigma_{ij}$  of  $H_t$ . The black lines denote the average decrease in  $\sigma_{ij}$  (fixed effect), the blue*  
 672 *dashed lines denote the heterogeneity of the average casual effect of N-back (95% Credible*  
 673 *Intervals) and the red solid lines denote the population heterogeneity of the effect of N-back.*  
 674 *The right panel shows the distribution of the individual effects of N-back on  $\sigma_{ij}$  of  $H_t$  in the*  
 675 *population predicted by the model. 76% of the population are predicted to demonstrate*  
 676 *increases in  $\sigma_{ij}$  of  $H_t$  when completing the N-back task.*

677 These findings provide further credence to the assessment of  $H_t$  made in the previous section.  
 678 Both  $\mu_{ij}$  and  $\sigma_{ij}$  of  $H_t$  change as a function of N-back. However, changes in  $\sigma_{ij}$  are predicted  
 679 to be more consistent across the population.

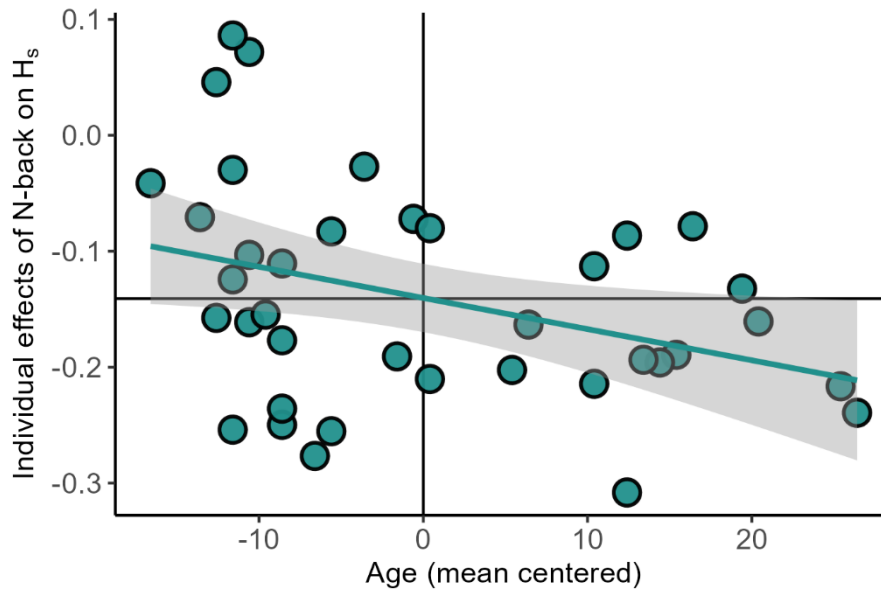
### 680 3.4 Understanding heterogeneity in average causal effect

681 Thus far it has been demonstrated that the mean of  $H_s$  and  $H_t$  change as a function of N-back.  
682 However, they both also demonstrate substantial variation across the sample, albeit in differing  
683 manners.  $H_s$  decreases for a majority of the sample but at varying magnitudes. Conversely,  $H_t$   
684 decreases for only two thirds of the sample with the remaining participants showing null effects  
685 or small reversals. Whilst this is theoretically useful, it is also important to understand *why*  
686 these effects are so variable. One possible explanation for entropic gaze metrics is age. Schieber  
687 & Gilland (2008) found that  $H_t$  consistently decreased as secondary task load increased, and  
688 these effects were exacerbated for older (67–86 years old) versus younger (19-35 years old)  
689 drivers. Schieber & Gilland (2008) proposed that this could be explained by shortfalls in visual-  
690 spatial resources of older drivers. A combination of loading these resources with a secondary  
691 task, and the demands of visual scanning during driving, could result in diminished scanning  
692 complexity under the interpretation of Wickens' (2020) Multiple Resource Theory model.  
693 More recent research supports this notion, suggesting that age-related impairments of top-down  
694 attentional control can exacerbate the effects that secondary cognitive tasks have on  $H_t$   
695 (Gazzaley et al, 2005; Shiferaw et al, 2019).

696 To investigate whether age-related impairments of top-down attentional control influence the  
697 effect of N-back, an additional model parameter  $\beta_A$  specifying the effect of age and its  
698 interaction with N-back was included for models of  $H_s$  and  $H_t$ . For  $H_s$ , the model predicted  
699 that age accounts for 9.9% of the between-participants heterogeneity in the causal effect of N-  
700 back (see Figure 14). A closer look at Figure 15 highlights that younger than average drivers  
701 still had decreases in gaze dispersion during N-back, although they were slightly smaller versus  
702 older than average drivers.

703

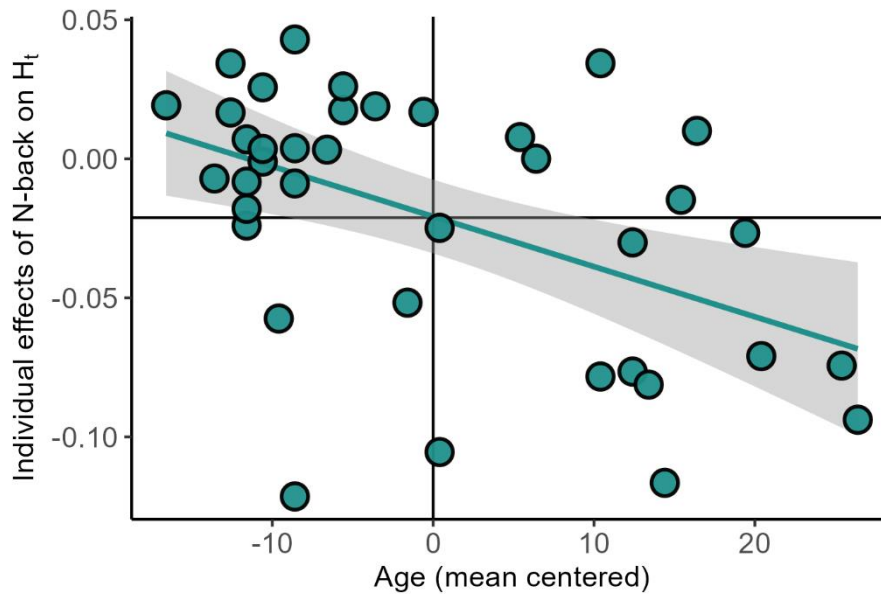
704



715 *Figure 14: Individual effects of N-back on  $H_s$  plotted against mean centred age. X axis vertical*  
 716 *line denotes mean age, y axis horizontal line denotes the average effect of N-back. All people*  
 717 *in the sample show decreases in gaze dispersion due to N-back. However, this effect is more*  
 718 *prominent for older than average people.*

719 As for  $H_t$ , the model predicts that driver age accounts for 19% of between-participants  
 720 heterogeneity in the causal effect of N-back. This suggests that age had a larger impact on how  
 721 N-back effected  $H_t$  in comparison to how it impacted  $H_s$ . Furthermore, how the between-  
 722 participants variance manifested was different. Younger than average drivers tended to show  
 723 null effects or even small reversals of the average causal effect, whereas older drivers observed  
 724 large reductions in  $H_t$  attributed to the effect of the N-back task (see Figure 15).

725  
 726  
 727  
 728  
 729  
 730  
 731  
 732



733  
734  
735  
736  
737  
738  
739  
740  
741  
742

743 *Figure 15: Individual effects of N-back  $H_t$  on plotted again mean centered age. X axis vertical*  
744 *line denotes mean age, y axis horizontal line denotes the average effect of N-back. Young than*  
745 *average people appear to have almost no effect of N-back on  $H_t$ , with even some slight*  
746 *reversals. Conversely, older than average people tend to have stronger than average effects of*  
747 *N-back on  $H_t$ .*

748 **4 Discussion**

749 The aim of this study was to investigate whether gaze metrics based on Information Theory  
750 could be used to estimate mental workload during hands-off Level 2 automated driving. Drivers  
751 had to monitor a road environment before taking over during critical and non-critical situations.  
752 The data presented in this manuscript focused on whether changes in eye movements during  
753 automated driving were associated with changes in mental workload. The observed data  
754 revealed that  $H_s$  was a reliable indicator of mental workload; the model predicted that 92% of  
755 the population would have decreases in  $H_s$  when completing the N-back task. Despite this,  
756 there was substantial variability in the size of the effect, with some people predicted to exhibit  
757 effects more than double the size of the average causal effect. Conversely, in contrast to  
758 previous work (Schieber & Gilland, 2008)  $H_t$  was found to be much less reliable for detecting

759 mental workload. Although the model predicted average reductions in gaze transition  
760 complexity for high workload conditions, only 66% of the population would exhibit similar  
761 decreases in  $H_t$  during N-back. Participant age appeared to be a strong predictor for how N-  
762 back influenced gaze entropic measures, accounting for 9.5% and 19% of the between-  
763 participants heterogeneity in the causal effect of N-back on  $H_s$  and  $H_t$ , respectively.

764 The current manuscript supports previous work that gaze dispersion reduces when mental  
765 workload increases (Reimer et al, 2009; 2010; Louw & Merat, 2017; Wilkie et al, 2019). The  
766 analysis also aligns with previous work that gaze complexity decreases under high mental  
767 workload (Schieber & Gilland, 2008). However, the analytic approach employed in this paper  
768 improves upon previous work by explicitly modelling and quantifying a key assumption of  
769 human behaviour; that people are inherently heterogenous. To build theories of psychological  
770 processes that inform eye movements during partial and conditional automated driving, it is  
771 advisable to take into account the heterogeneity of the sample (Bogler et al, 2019). This is  
772 especially vital when heterogeneity is sufficient such that null effects or reversals are observed  
773 in the data (Bogler et al, 2019). In the current manuscript, this was observed for  $H_t$  as a function  
774 of N-back. Under the assumption that this variance is not due to poor experimental control,  
775 such theories will need to include subpopulations that differ in causal processes. One previous  
776 attempt at this approach was by Reimer et al (2009) who considered the pattern of visual  
777 tunneling under high mental workload in the population by computing change scores from pre-  
778 task periods of gaze dispersion for each individual. Although this identifies whether individuals  
779 in the sample follow average trends, it does not generate a population distribution of the effects  
780 of mental workload on eye movements. Instead, the current manuscript constructed a  
781 population heterogeneity distribution implied by the models estimate of the population mean  
782 ( $\mu$ ) and standard deviation ( $\sigma$ ) for each gaze entropic metric.

783 The effect of N-back on  $H_s$  and  $H_t$  differed as function of age, albeit in slightly different ways.  
784 For  $H_s$ , a majority of the sample showed reductions in the spatial distribution of gaze as a  
785 function of N-back; this reduction was weaker for younger than average participants.  
786 Conversely, for  $H_t$  there was no effect of N-back for the younger than average sample. There  
787 were even small *increases* in gaze complexity when completing the N-back. The older than  
788 average drivers showed a strong decrease in gaze transition complexity. It is important to note  
789 that age had minimal effects on  $H_s$  and  $H_t$  directly; rather, age influenced how much N-back  
790 affected gaze. In this sense, the current findings support previous work that report the lack of  
791 a direct effect of age on gaze centralization (Reimer et al, 2010; 2012). One explanation for the  
792 indirect effect of age on gaze entropy could be due to a healthy age-related cognitive decline.  
793 Top-down modulation underlies selective attention by suppressing the neural activity  
794 associated with the interference of task irrelevant representations (Gazzaley et al, 2005; Ploner  
795 et al, 2001). In the context of gaze control, top-down modulation also allows for efficient  
796 sampling of the environment by overriding bottom-up input, thus allowing drivers to efficiently  
797 monitor dynamic scenes (Shiferaw et al, 2019). However, research has found that older  
798 populations struggle to suppress task irrelevant information (Gazzaley et al, 2005).  
799 Consequently, this combination leads to a reduction in scanning complexity due to the  
800 interference of the N-back task, in combination with already weakened top-down selective  
801 attention processes of older than average participants.

802 In terms of their implications, these results can provide DMS designers with some important  
803 principles for using the correct metrics for detecting mental workload. A key aspect to be  
804 considered is that driver demographics should be taken into account when using DMS to  
805 establish driver state in vehicles. This manuscript clearly demonstrates that age influenced the  
806 extent to which N-back changed gaze-based metrics. As such, if DMS were to use  $H_s$  as an  
807 indicator of mental workload, differing thresholds might be necessary for drivers of different

808 ages. For example, it might be necessary for a smaller threshold in the reduction of spatial  
809 dispersion for younger drivers as their gaze might be less effected by N-back, even though they  
810 might be experiencing high levels of mental workload, which could, in turn, impair their  
811 takeover performance. Another element to for DMS engineers to consider is which parameter  
812 of the gaze metric distribution should be used to establish a change in driver state. The current  
813 state of the art assumes that changes in central tendency should be used (e.g. a change in mean  
814  $H_t$  establishes that N-back induces high mental workload). However, the current findings  
815 suggest that changes in *variance* may be more reliable. Increases in the trial-by-trial variance  
816 of  $H_t$  were predicted to be found in 76% of the population during high mental workload; only  
817 66% of the population were predicted to follow average trends regarding a change in mean  $H_t$ .  
818 This suggests that changes in the variance of gaze complexity were more reliable than changes  
819 in the mean. High trial-by-trial variance during N-back suggests that drivers had frequent  
820 fluctuations in the complexity of their gaze from one trial to the next. Rather than finding an  
821 optimal level of gaze transitions that were suitable for all trials, the randomness of the  
822 transitions changed frequently. It has been proposed that the motor controls involved in eye  
823 movements aim to optimize inference (Parr & Friston, 2017) which implies that there are  
824 optimal levels of  $H_t$  to sample the environment efficiently (Shiferaw et al, 2019). Hence the  
825 results in the current manuscript suggest that high mental workload disrupts this eye movement  
826 optimization, resulting in variable, inefficient monitoring of the driving environment. The  
827 utilization of variance as an indicator for mental workload supports results from research within  
828 the visual distraction domain. These show, for example, that presentation of information by  
829 certain in-vehicle information systems reduces variations in fixation durations, supporting  
830 more efficient information processing (Horrey & Wickens, 2007; Kujala & Saarilouma, 2011).  
831 A similar suggestion is made here; without N-back trial-by-trial variance is small suggesting  
832 drivers establish and optimal  $H_t$  that allows them to efficiently sample the road. As mental

833 workload increases, so does the variance in  $H_t$ , which is proposed as an indicator for visual  
834 scanning inefficiency. These findings suggest more research is needed to understand whether  
835 different parameters of response distributions can be used as indicators of mental workload.

836 Another interesting result from this study was the effect of lead vehicle presence. There was a  
837 small but consistent decrease in the spatial distribution of gaze for trials with lead vehicles.  
838 This supports previous research that drivers reduce the spread of their gaze and reallocate  
839 attention towards lead vehicles (Crundall et al, 2004). A key difference is that Crundall et al  
840 (2004) observed reductions in gaze dispersion only when instructing drivers to follow a lead  
841 vehicle during manual driving. Conversely, participants in the current study were instructed to  
842 monitor the entire road environment for hazards. Despite this request, the lead vehicle was  
843 clearly a salient object within the road environment and thus likely attracted drivers' attention.  
844 This may pose a problem for DMS in the real world, given that gaze dispersion has been shown  
845 to decrease in the presence of a lead vehicle, irrespective of increasing mental workload.  
846 Therefore, DMS will need to ensure that it can distinguish between drivers attending towards  
847 vehicles on the road ahead, and those under increased mental workload. It should be noted that  
848 the average reduction in gaze dispersion was much smaller for lead vehicles versus N-back  
849 conditions, however this still will not disentangle drivers who had smaller reductions in gaze  
850 dispersion during N-back conditions.

851 One limitation of the current work is that these model predictions need to be validated on a  
852 wider range of datasets. A statistical model is only as good as the data used to fit it. Whilst age  
853 ranges and gender balance were representative in the current sample, they mostly represented  
854 white, British drivers in the north of England. As such, whether their behaviours translate well  
855 to drivers from different cultures remains to be seen. Another limitation with the current work  
856 is the use of a Gaussian distribution as the likelihood for the modelling. Whilst the data were  
857 approximated by a Gaussian distribution, and the posterior predictive checks appear to fit the



858 data well, normalized  $H_s$  and  $H_t$  are technically continuous variables bounded between 0 and  
859 1. Conversely, any value is possible for a Gaussian distribution. The Beta distribution is a  
860 candidate that might be better suited for modelling these types of variables (Paolino, 2001;  
861 Ferrari & Cribari-Neto, 2004). Whilst a comparison of Gaussian and Beta likelihoods on  
862 clinical data highlighted that the estimates were very similar (Kurz, 2023) the Beta distribution  
863 is a better conceptual fit and produced slightly more precise estimates. Future research may  
864 compare these methods to investigate any differences in the context of gaze metrics.

865 In conclusion, Information Theoretic eye-based metrics have shown some promise in  
866 identifying increased mental workload in drivers engaging in an N-back task during hands-off  
867 Level 2 automated driving. Both  $H_s$  (Pillai et al, 2022) and  $H_t$  (Schieber & Gilland, 2008)  
868 were found to decrease as a function of increasing task load. However, the current research  
869 suggests that this assessment is incomplete. Whilst the average trends are consistent with  
870 previous research, there is substantial variance in how eye movements change as a function of  
871 task load across a population. For future DMS systems that apply to a multitude of drivers, this  
872 variance needs to be properly measured and quantified. One potential source of this  
873 heterogeneity is age, and thus DMS designers should consider how their input metrics are  
874 influenced by differing demographic variables.

875

876

877

878

879

880

881 **References**

- 882 Bolger, N., Zee, K. S., Rossignac-Milon, M., & Hassin, R. R. (2019). Causal processes in  
883 psychology are heterogeneous. *Journal of Experimental Psychology: General*, *148*(4), 601.
- 884 Bottos, S., & Balasingam, B. (2020). Tracking the progression of reading using eye-gaze point  
885 measurements and hidden markov models. *IEEE Transactions on Instrumentation and*  
886 *Measurement*, *69*(10), 7857-7868.
- 887 Brookhuis, K. A., & De Waard, D. (1993). The use of psychophysiology to assess driver  
888 status. *Ergonomics*, *36*(9), 1099-1110.
- 889 Brookhuis, K. A., & de Waard, D. (2000). Assessment of drivers' workload: Performance and  
890 subjective and physiological indexes. In *Stress, workload, and fatigue* (pp. 321-333). CRC  
891 press.
- 892 Bruggen, A. (2015). An empirical investigation of the relationship between workload and  
893 performance. *Management Decision*, *53*(10), 2377-2389.
- 894 Bürkner, P. C. (2017). Advanced Bayesian multilevel modeling with the R package  
895 brms. *arXiv preprint arXiv:1705.11123*.
- 896 Carsten, O., Lai, F. C., Barnard, Y., Jamson, A. H., & Merat, N. (2012). Control task  
897 substitution in semiautomated driving: Does it matter what aspects are automated?. *Human*  
898 *factors*, *54*(5), 747-761.
- 899 Chen, W., Sawaragi, T., & Hiraoka, T. (2022). Comparing eye-tracking metrics of mental  
900 workload caused by NDRTs in semi-autonomous driving. *Transportation research part F:*  
901 *traffic psychology and behaviour*, *89*, 109-128.
- 902 Clark, A. (2013). Whatever next? Predictive brains, situated agents, and the future of cognitive  
903 science. *Behavioral and brain sciences*, *36*(3), 181-204.

904 Crundall, D., Shenton, C., & Underwood, G. (2004). Eye movements during intentional car  
905 following. *Perception*, 33(8), 975-986.

906 da Silva, F. P. (2014). Mental workload, task demand and driving performance: what  
907 relation?. *Procedia-Social and Behavioral Sciences*, 162, 310-319.

908 De Waard, D., & Brookhuis, K. A. (1996). The measurement of drivers' mental workload.

909 De Winter, J. C., Happee, R., Martens, M. H., & Stanton, N. A. (2014). Effects of adaptive  
910 cruise control and highly automated driving on workload and situation awareness: A review of  
911 the empirical evidence. *Transportation research part F: traffic psychology and behaviour*, 27,  
912 196-217.

913 Di Stasi, L. L., Díaz-Piedra, C., Ruiz-Rabelo, J. F., Rieiro, H., Carrion, J. M. S., & Catena, A.  
914 (2017). Quantifying the cognitive cost of laparo-endoscopic single-site surgeries: Gaze-based  
915 indices. *Applied Ergonomics*, 65, 168-174.

916 Ellis, S. R., & Stark, L. (1986). Statistical dependency in visual scanning. *Human*  
917 *factors*, 28(4), 421-438.

918 Engström, J., Markkula, G., Victor, T., & Merat, N. (2017). Effects of cognitive load on driving  
919 performance: The cognitive control hypothesis. *Human factors*, 59(5), 734-764.

920 Ferrari, S., & Cribari-Neto, F. (2004). Beta regression for modelling rates and  
921 proportions. *Journal of applied statistics*, 31(7), 799-815.

922 Fuller, R. (2005). Towards a general theory of driver behaviour. *Accident analysis &*  
923 *prevention*, 37(3), 461-472.

924 Gazzaley, A., Cooney, J. W., Rissman, J., & D'esposito, M. (2005). Top-down suppression  
925 deficit underlies working memory impairment in normal aging. *Nature neuroscience*, 8(10),  
926 1298-1300.

927 Gold, C., Berisha, I., & Bengler, K. (2015, September). Utilization of drivetime–performing  
928 non-driving related tasks while driving highly automated. In *Proceedings of the Human*  
929 *Factors and Ergonomics Society Annual Meeting* (Vol. 59, No. 1, pp. 1666-1670). Sage CA:  
930 Los Angeles, CA: SAGE Publications.

931 Gold, C., Damböck, D., Bengler, K., & Lorenz, L. (2013). Partially automated driving as a  
932 fallback level of high automation. In *6. tagung fahrerassistenzsysteme*.

933 Henderson, J. M. (2003). Human gaze control during real-world scene perception. *Trends in*  
934 *cognitive sciences*, 7(11), 498-504.

935 Henderson, J. M. (2017). Gaze control as prediction. *Trends in cognitive sciences*, 21(1), 15-  
936 23.

937 Holmqvist, K., Nyström, M., Andersson, R., Dewhurst, R., Jarodzka, H., & Van de Weijer, J.  
938 (2011). *Eye tracking: A comprehensive guide to methods and measures*. OUP Oxford.

939 Horrey, W. J., & Wickens, C. D. (2007). In-vehicle glance duration: distributions, tails, and  
940 model of crash risk. *Transportation research record*, 2018(1), 22-28.

941 Krejtz, K., Duchowski, A., Szmids, T., Krejtz, I., González Perilli, F., Pires, A., ... & Villalobos,  
942 N. (2015). Gaze transition entropy. *ACM Transactions on Applied Perception (TAP)*, 13(1), 1-  
943 20.

944 Krejtz, K., Szmids, T., Duchowski, A. T., & Krejtz, I. (2014, March). Entropy-based statistical  
945 analysis of eye movement transitions. In *Proceedings of the Symposium on Eye Tracking*  
946 *Research and Applications* (pp. 159-166).

947 Kruschke, J. (2014). Doing Bayesian data analysis: A tutorial with R, JAGS, and Stan.

948 Kujala, T., & Saariluoma, P. (2011). Effects of menu structure and touch screen scrolling style  
949 on the variability of glance durations during in-vehicle visual search tasks. *Ergonomics*, *54*(8),  
950 716-732.

951 Kurz, S. (2023, June, 25). Causal inference with beta regression.  
952 ([https://solomonkurz.netlify.app/blog/2023-06-25-causal-inference-with-beta-regression/#ref-](https://solomonkurz.netlify.app/blog/2023-06-25-causal-inference-with-beta-regression/#ref-paolino2001maximum)  
953 [paolino2001maximum](https://solomonkurz.netlify.app/blog/2023-06-25-causal-inference-with-beta-regression/#ref-paolino2001maximum))

954 Lo, S., & Andrews, S. (2015). To transform or not to transform: Using generalized linear mixed  
955 models to analyse reaction time data. *Frontiers in psychology*, *6*, 1171.

956 Louw, T., & Merat, N. (2017). Are you in the loop? Using gaze dispersion to understand driver  
957 visual attention during vehicle automation. *Transportation Research Part C: Emerging*  
958 *Technologies*, *76*, 35-50.

959 Makowski, D., Ben-Shachar, M. S., & Lüdtke, D. (2019). bayestestR: Describing effects and  
960 their uncertainty, existence and significance within the Bayesian framework. *Journal of Open*  
961 *Source Software*, *4*(40), 1541.

962 Mehler, B., Reimer, B., & Dusek, J. A. (2011). MIT AgeLab delayed digit recall task (n-  
963 back). *Cambridge, MA: Massachusetts Institute of Technology*, *17*.

964 Mok, B., Johns, M., Lee, K. J., Miller, D., Sirkin, D., Ive, P., & Ju, W. (2015, September).  
965 Emergency, automation off: Unstructured transition timing for distracted drivers of automated  
966 vehicles. In *2015 IEEE 18th international conference on intelligent transportation systems* (pp.  
967 2458-2464). IEEE.

968 Mole, C., Pekkanen, J., Sheppard, W., Louw, T., Romano, R., Merat, N., ... & Wilkie, R.  
969 (2020). Predicting takeover response to silent automated vehicle failures. *Plos one*, *15*(11),  
970 e0242825.

971 Öztürk, İ., Merat, N., Rowe, R., & Fotios, S. (2023). The effect of cognitive load on Detection-  
972 Response Task (DRT) performance during day-and night-time driving: A driving simulator  
973 study with young and older drivers. *Transportation research part F: traffic psychology and*  
974 *behaviour*, 97, 155-169.

975 Paolino, P. (2001). Maximum likelihood estimation of models with beta-distributed dependent  
976 variables. *Political Analysis*, 9(4), 325-346.

977 Parr, T., & Friston, K. J. (2017). Working memory, attention, and salience in active  
978 inference. *Scientific reports*, 7(1), 14678.

979 Pillai, P., Balasingam, B., Kim, Y. H., Lee, C., & Biondi, F. (2022). Eye-gaze metrics for  
980 cognitive load detection on a driving simulator. *IEEE/ASME Transactions on*  
981 *Mechatronics*, 27(4), 2134-2141.

982 Ploner, C. J., Ostendorf, F., Brandt, S. A., Gaymard, B. M., Rivaud-Péchoux, S., Ploner, M.,  
983 ... & Pierrot-Deseilligny, C. (2001). Behavioural relevance modulates access to spatial working  
984 memory in humans. *European Journal of Neuroscience*, 13(2), 357-363.

985 Radlmayr, J., Fischer, F. M., & Bengler, K. (2019). The influence of non-driving related tasks  
986 on driver availability in the context of conditionally automated driving. In *Proceedings of the*  
987 *20th Congress of the International Ergonomics Association (IEA 2018) Volume VI: Transport*  
988 *Ergonomics and Human Factors (TEHF), Aerospace Human Factors and Ergonomics 20* (pp.  
989 295-304). Springer International Publishing.

990 Raptis, G. E., Fidas, C. A., & Avouris, N. M. (2017, May). On implicit elicitation of cognitive  
991 strategies using gaze transition entropies in pattern recognition tasks. In *Proceedings of the*  
992 *2017 CHI Conference Extended Abstracts on Human Factors in Computing Systems* (pp. 1993-  
993 2000).

994 Reimer, B. (2009). Impact of cognitive task complexity on drivers' visual  
995 tunneling. *Transportation Research Record*, 2138(1), 13-19.

996 Reimer, B., Mehler, B., Wang, Y., & Coughlin, J. F. (2010, September). The impact of  
997 systematic variation of cognitive demand on drivers' visual attention across multiple age  
998 groups. In *Proceedings of the Human Factors and Ergonomics Society Annual Meeting* (Vol.  
999 54, No. 24, pp. 2052-2055). Sage CA: Los Angeles, CA: SAGE Publications.

1000 Reimer, B., Mehler, B., Wang, Y., & Coughlin, J. F. (2012). A field study on the impact of  
1001 variations in short-term memory demands on drivers' visual attention and driving performance  
1002 across three age groups. *Human factors*, 54(3), 454-468.

1003 Schieber, F., & Gilland, J. (2008, September). Visual entropy metric reveals differences in  
1004 drivers' eye gaze complexity across variations in age and subsidiary task load. In *Proceedings*  
1005 *of the Human Factors and Ergonomics Society Annual Meeting* (Vol. 52, No. 23, pp. 1883-  
1006 1887). Sage CA: Los Angeles, CA: SAGE Publications.

1007 Schielzeth, H., Dingemanse, N. J., Nakagawa, S., Westneat, D. F., Allogue, H., Teplitsky, C.,  
1008 ... & Araya-Ajoy, Y. G. (2020). Robustness of linear mixed-effects models to violations of  
1009 distributional assumptions. *Methods in ecology and evolution*, 11(9), 1141-1152.

1010 Shannon, C. E. (1948). A mathematical theory of communication. *The Bell system technical*  
1011 *journal*, 27(3), 379-423.

1012 Shiferaw, B., Downey, L., & Crewther, D. (2019). A review of gaze entropy as a measure of  
1013 visual scanning efficiency. *Neuroscience & Biobehavioral Reviews*, 96, 353-366.

1014 Sodhi, M., Reimer, B., & Llamazares, I. (2002). Glance analysis of driver eye movements to  
1015 evaluate distraction. *Behavior Research Methods, Instruments, & Computers*, 34, 529-538.

1016 Spratling, M. W. (2017). A predictive coding model of gaze shifts and the underlying  
1017 neurophysiology. *Visual Cognition*, 25(7-8), 770-801.

1018 Standard, S. (2018). J3016B: Taxonomy and Definitions for Terms Related to Driving  
1019 Automation Systems for On-Road Motor Vehicles-SAE International.

1020 Tatler, B. W., Brockmole, J. R., & Carpenter, R. H. (2017). LATEST: A model of saccadic  
1021 decisions in space and time. *Psychological review*, 124(3), 267.

1022 Vehtari, A., Gelman, A., & Gabry, J. (2017). Practical Bayesian model evaluation using leave-  
1023 one-out cross-validation and WAIC. *Statistics and computing*, 27, 1413-1432.

1024 Velichkovsky, B., Sprenger, A., & Unema, P. (1997). Towards gaze-mediated interaction:  
1025 Collecting solutions of the “Midas touch problem”. In *Human-Computer Interaction*  
1026 *INTERACT'97: IFIP TC13 International Conference on Human-Computer Interaction, 14th–*  
1027 *18th July 1997, Sydney, Australia* (pp. 509-516). Springer US.

1028 Wang, Y., Reimer, B., Dobres, J., & Mehler, B. (2014). The sensitivity of different  
1029 methodologies for characterizing drivers’ gaze concentration under increased cognitive  
1030 demand. *Transportation research part F: traffic psychology and behaviour*, 26, 227-237.

1031 Weiss, R. S., Remington, R., & Ellis, S. R. (1989). Sampling distributions of the entropy in  
1032 visual scanning. *Behavior Research Methods, Instruments, & Computers*, 21(3), 348-352.

1033 Wickens, C. D. (2002). Multiple resources and performance prediction. *Theoretical issues in*  
1034 *ergonomics science*, 3(2), 159-177.

1035 Wickens, C. D. (2020). Processing resources and attention. In *Multiple task performance* (pp.  
1036 3-34). CRC Press.



1037 Wilkie, R., Mole, C., Giles, O., Merat, N., Romano, R., & Makkula, G. (2019, June). Cognitive  
1038 load during automation affects gaze behaviours and transitions to manual steering control.  
1039 In *Driving Assessment Conference* (Vol. 10, No. 2019). University of Iowa.

1040 Young, M. S., & Stanton, N. A. (2002). Malleable attentional resources theory: a new  
1041 explanation for the effects of mental underload on performance. *Human factors*, 44(3), 365-  
1042 375.

1043 Zeeb, K., Buchner, A., & Schrauf, M. (2016). Is take-over time all that matters? The impact of  
1044 visual-cognitive load on driver take-over quality after conditionally automated  
1045 driving. *Accident analysis & prevention*, 92, 230-239.

1046

1047

1048

1049

1050

1051

1052

1053